Table I. Predictive marker genes for drug-induced cytotoxicity.

A) Genes known as drug sensitivity determinants.

Gene		Correlation coefficient (R)				
		5-FU	DOX	CDDP	CPT-11	SN-38
BCL2	cDNA		-			
	Oligo		0.505[b]			
	PCR		0.423[b]			
DPYD	cDNA	-				
	Oligo	0.475[b]				
	PCR	0.682[b]				
GSTP1	cDNA			-0.525[b]		
	Oligo			-0.430[c]		
	PCR			-0.426[c]		
MGMT	cDNA					-
	Oligo					0.412[c]
	PCR					0.538[b]
XRCC1	cDNA				0.589[b]	0.459[b]
	Oligo				-	-
	PCR				0.525[b]	0.392[c]

B) The highest correlative genes for drug sensitivity.

Gene		Correlation coefficient (R)				
		5-FU	DOX	CDDP	CPT-11	SN-38
ARFRP1	cDNA			0.615[a]		
	Oligo			0.565[a]		
	PCR			0.440[c]		
B4GALT5	cDNA	0.632[a]				
	Oligo	0.662[a]				
	PCR	0.772[a]				
CALU	cDNA				0.577[a]	
	Oligo				0.577[a]	
	PCR				0.423[c]	
IFITM1	cDNA			-0.630[a]		
	Oligo			-0.734[a]		
	PCR			-0.567[a]		
KIAA0685	cDNA			-0.567[a]		
	Oligo			-0.570[a]		
	PCR			-0.462[b]		
NRCAM	cDNA		0.645[a]			
	Oligo		0.653[a]			
	PCR		0.493[b]			
SIPA1L2	cDNA			-0.737[a]		
	Oligo			-0.595[a]		
	PCR			-0.499[b]		
UGCG	cDNA	0.579[a]				
	Oligo	0.578[a]				
	PCR	0.656[a]				
XBP1	cDNA	0.776[a]				
	Oligo	0.569[a]				
	PCR	0.804[a]				

cDNA, cDNA microarray analysis; oligo, oligonucleotide array analysis; PCR, real-time RT-PCR (linear regression analysis); [a]$p<0.01$; [b]$0.01 \leq p<0.05$; [c]$0.05 \leq p<0.1$.

markers: The numbers were 30 for 5-FU, 43 for MMC, 78 for DOX, 38 for CDDP, 41 for TXL, 43 for TXT, 30 for CPT-11, and 56 for SN-38 ($p<0.05$).

Determination of prediction marker genes using real-time RT-PCR. The aim was to determine reliable prediction markers for 8 drugs from each of the 359 candidates. First, we focused on 50 genes whose functions as drug sensitivity factors had been clearly demonstrated in at least 2 reports among a total of 897 related papers (11), but the 359 candidates included very few genes known as drug sensitivity determinants. Although we extended the screening field to a range of $p<0.1$ in either cDNA or oligonucleotide microarray screening, no possible markers were found for TXL- and TXT-induced cytotoxicity, and the number of selected genes was only 11: *DPYD* (dihydropyrimidine dehydrogenase gene) and *UMPS* (uridine monophosphate synthetase gene) for 5-FU; *ABCB1* (ATP-binding cassette, sub-family B, member 1 gene) for MMC; *MYC* (v-myc avian myelocytomatosis viral oncogene homolog) and *BCL2* (B-cell CLL/lymphoma 2 gene) for DOX, *GSTP1* (glutathione S-transferase π1 gene) and *GCLC* (glutamate-cysteine ligase, catalytic subunit gene) for CDDP; *TOP1* (topo-isomerase I gene) and *XRCC1* (X-ray repair complementing defective repair in Chinese hamster cells 1 gene) for CPT-11; *MGMT* (O^6-methylguanine-DNA methyltransferase gene), and *POR* [P-450 (cytochrome) reductase gene], *TOP1*, and *XRCC1* for SN-38 (16-37). These selected candidates were subjected to real-time RT-PCR analysis and we confirmed only 5 correlations: *DPYD* with 5-FU, *BCL2* with DOX, *GSTP*1 with CDDP, *XRCC1* with CPT-11, and *MGMT* with SN-38, even when the selection criterion was determined as $p<0.1$ in the linear regression analysis (Table IA).

The very small number of marker genes for limited drugs encouraged us to select additional potent marker genes via another approach, using only the data of expression-sensitivity correlation analysis. We selected genes which highly correlated with drug efficacy in the expression levels ($p<0.01$) in both array screenings. A total of 20 genes among 359 candidates satisfied the selection criteria, and 9 genes were finally selected as the most potent markers of sensitivity to 4 drugs after the confirmation of correlations by real-time RT-PCR ($p<0.1$). They were *B4GALT5* (UDP-Gal: ßGlcNAc ß 1,4-galactosyl-transferase, polypeptide 5 gene), *UGCG* (UDP-glucose ceramide glucosyltransferase gene), and *XBP1* (X-box binding protein 1 gene) for 5-FU, *NRCAM* (neuronal cell adhesion molecule gene) for DOX, *ARFRP1* (ADP-ribosylation factor related protein 1 gene), *IFITM1* (interferon induced trans-membrane protein 1 gene), *KIAA0685*, and *SIPA1L2* (signal-induced proliferation-associated 1 like 2 gene) for CDDP, and *CALU* (calumenin gene) for CPT-11 (Table IB). Despite the relatively increased number of potent marker genes, no possible marker genes of MMC-, TXL-, TXT-, or additionally SN-38-induced cytotoxicity were revealed in this approach.

Prediction formulae of sensitivity to 4 drugs in vitro. Selection of the truly significant genes for sensitivities to drugs would allow us to predict therapeutic response to these agents simultaneously, at which point we could understand their interplay in the expression. We therefore attempted to develop such a prediction model using expression data of the selected genes, and performed multiple regression analysis to understand the interplay in the expression of the genes.

Table II. Explanatory variables (x_{ip}) and estimated coefficients (θ_p) in *in vitro* prediction formulae for drug-induced cytotoxicity.

A) Prediction formulae using 5 functionally known genes.

	θ_p				
x_{ip}	5-FU	DOX	CDDP	CPT-11	SN-38
ln [*BCL2*]	0.071	0.159	-0.468	0.086	0.139
	(0.300)	(0.015)	(0.001)	(0.041)	(0.380)
ln [*DPYD*]	0.108	0.029	-0.032	0.007	0.036
	(0.000)[b]	(0.039)	(0.316)	(0.404)	(0.277)
ln [*GSTP1*]	0.138	-0.036	-0.325	-0.052	-0.221
	(0.057)	(0.576)	(0.026)	(0.217)	(0.163)
ln [*MGMT*]	-0.000[a]	0.012	0.022	0.002	0.046
	(0.849)	(0.006)	(0.022)	(0.382)	(0.000)[b]
ln [*XRCC1*]	-0.115	-0.104	0.066	0.215	0.390
	(0.249)	(0.256)	(0.762)	(0.001)	(0.091)
ε_i	5.730	3.724	6.125	7.793	2.394

B) Prediction formulae using 9 highly correlative genes.

	θ_p				
X_{ip}	5-FU	DOX	CDDP	CPT-11	SN-38
ln [*ARFRP1*]	-0.237	-0.127	0.712	-0.213	
	(0.101)	(0.305)	(0.006)	(0.005)	
ln [*B4GALT5*]	0.352	0.065	-0.231	-0.035	
	(0.064)	(0.661)	(0.580)	(0.675)	
ln [*CALU*]	-0.258	-0.075	-0.347	0.178	
	(0.215)	(0.676)	(0.314)	(0.082)	
ln [*IFITM1*]	-0.165	-0.058	-0.274	-0.016	
	(0.030)	(0.341)	(0.043)	(0.649)	
ln [*KIAA0685*]	0.294	0.366	-0.708	-0.016	
	(0.342)	(0.192)	(0.221)	(0.918)	
ln [*NRCAM*]	0.087	0.145	-0.045	0.046	
	(0.052)	(0.000)[b]	(0.565)	(0.027)	
ln [*SIPA1L2*]	-0.044	-0.090	0.039	0.041	
	(0.436)	(0.051)	(0.758)	(0.120)	
ln [*UGCG*]	0.470	-0.081	-0.164	0.145	
	(0.030)	(0.631)	(0.678)	(0.152)	
ln [*XBP1*]	0.087	-0.068	0.864	-0.254	
	(0.676)	(0.679)	(0.038)	(0.012)	
ε_i	5.243	3.745	5.518	8.158	

[ ], expression level of indicated gene; [a]-0.000: -0.0008852; ( ), p-value; [b]0.000: <0.0005.

The expression levels of the selected genes quantified by real-time RT-PCR and cellular sensitivity to drugs (IC_{50} value for each drug) were used as the explanatory variables ($x_1, x_2, \cdots, x_p$) and the response variable (y), respectively, and we estimated ($\theta_1, \cdots, \theta_p$) of the formula in the linear model: $y_i = x_{i1}\theta_1 + x_{i2}\theta_2 + \cdots + x_{ip}\theta_p + \varepsilon_i$ ($i = 1, 2, \cdots, n$), where ε_i is a random error, using NLReg software.

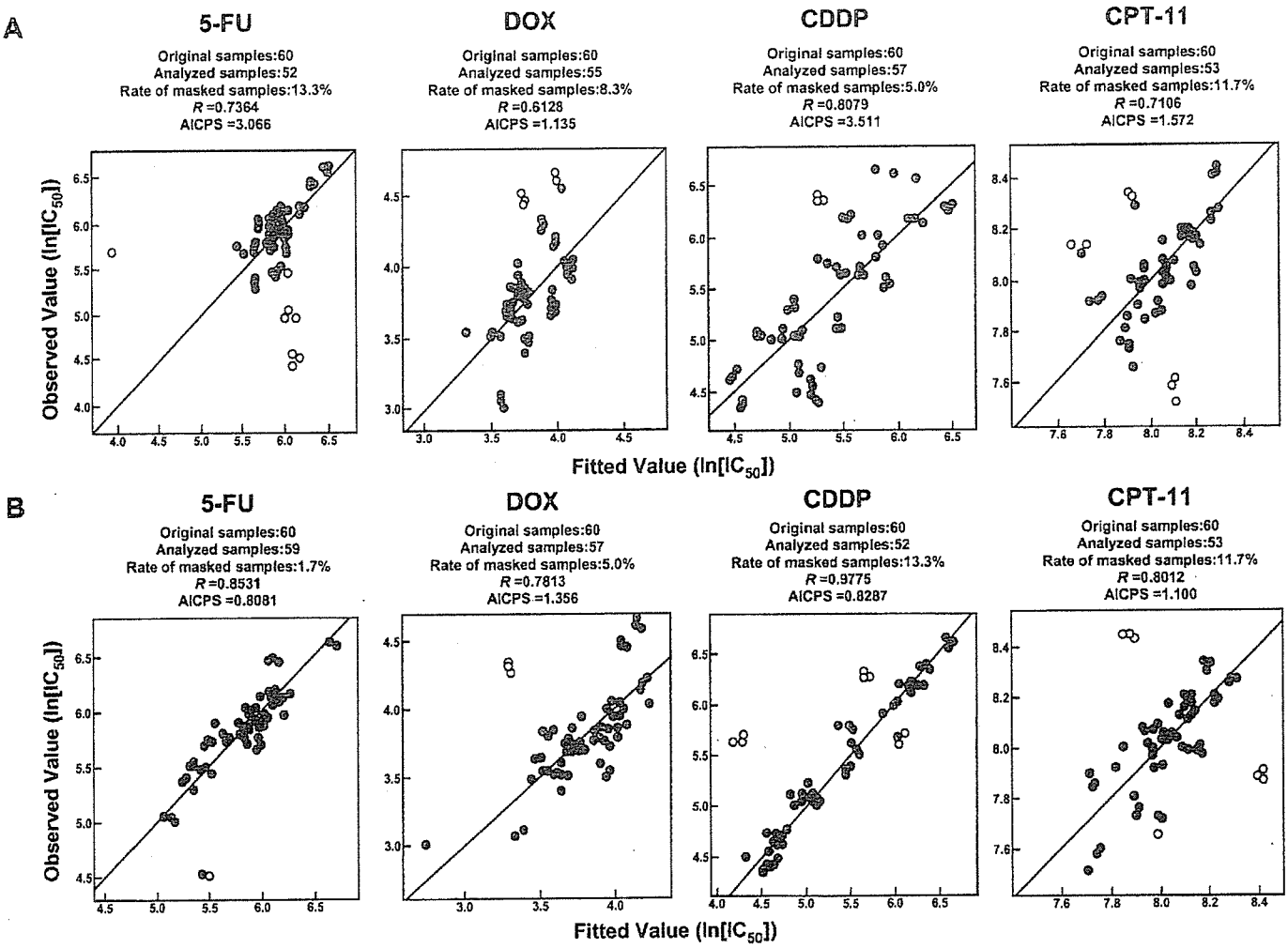

Figure 1. The relationship between observed IC_{50} value and fitted IC_{50} value calculated by fixed formulae for esophageal squamous cell carcinoma cell lines. We selected 5 functionally known genes for sensitivity to 5 drugs (A) and 9 highly correlative genes with sensitivity to 4 drugs in expression levels (B), as predictive marker genes through comprehensive gene expression analyses using cDNA and oligonucleotide microarrays and quantitative real-time RT-PCR. In this analysis, 60 independent data sets, composed by expression levels of selected genes and IC_{50} values for 20 KYSE cell lines, were used. A vertical axis and a horizontal axis show observed and fitted IC_{50} values (both are logarithmically transformed), respectively. A closed circle indicates analyzed sample data, while an open circle indicates a masked outlier.

These approaches provided 4 prediction formulae of drug sensitivity *in vitro* when we used 5 genes known as sensitivity determinants and 9 genes selected from expression-sensitivity correlation analysis alone. The obtained θ_p is shown with p-value in Table II. Since the lower p-value indicates lower probability in order to demonstrate that θ-value could be 0 in the prediction formula, genes showing lower p-values can be estimated as more important in drug sensitivity prediction: The expression level is of value as the explanatory variable in the formula. As expected, the genes previously suggested as important sensitivity determinant maintained their significance in drug sensitivity prediction, i.e. *DPYD* for 5-FU, *BCL2* for DOX, *GSTP1* for CDDP, *XRCC1* for CPT-11, and *MGMT* for SN-38 (Table IIA). The prediction formulae using expression data of 9 genes selected by expression-sensitivity correlation analysis alone also demonstrated that most of the selected genes played important roles in prediction: *B4GALT5* and *UGCG* for 5-FU; *NRCAM* for DOX; *ARFRP1* and *IFITM1* for CDDP; and *CALU* for CPT-11, despite some unexpected data such as *XBP1* for 5-FU, and *KIAA0685* and *SIPA1L2* for CDDP (Table IIB). A positive θ indicates that the corresponding explanatory variable, gene expression, acts as a resistant factor in the prediction formulae, while a negative θ indicates the inverse action of the variable. Nevertheless, the levels of θ-value do not directly account for the importance of the explanatory variable, since the expression levels of genes differ considerably from one another. All of the prediction formulae provided showed relatively high fitness, but the obtained correlation coefficients (R) and AIC for each sample (AICPS) suggested the limited value of the 4 formulae using 5 known sensitivity determinant genes in drug sensitivity prediction (Fig. 1A). The R-values and the AIPCS values were, respectively, lower and higher than those in the prediction formulae composed of 9 functionally unproven genes selected by expression-sensitivity correlation analysis alone (Fig. 1B).

Prediction model for clinical response to 5-FU-based chemotherapy. Using the same sets of genes, we attempted to construct a clinical application model through the investigation of clinical samples and their response data. Since 5-FU-based

Table III. Explanatory variables (x_{ip}) and estimated coefficients (θ_p) in prediction formulae for clinical response to 5-FU-based adjuvant chemotherapy.

A) Prediction formulae using 5 functionally known genes.

x_{ip}	θ_p	
	Overall survival	Disease-free survival
ln [*BCL2*]	-0.920 (0.110)	-1.105 (0.144)
ln [*DPYD*]	0.203 (0.604)	0.455 (0.389)
ln [*GSTP1*]	0.313 (0.726)	0.219 (0.853)
ln [*MGMT*]	0.863 (0.064)	1.100 (0.072)
ln [*XRCC1*]	0.451 (0.300)	0.426 (0.451)
ε_i	5.398	4.954

B) Prediction formulae using 9 highly correlative genes.

x_{ip}	θ_p	
	Overall survival	Disease-free survival
ln [*ARFRP1*]	0.669 (0.744)	0.852 (0.722)
ln [*B4GALT5*]	0.125 (0.928)	0.336 (0.836)
ln [*CALU*]	-0.115 (0.936)	-0.298 (0.859)
ln [*IFITM1*]	0.000[a] (1.000)	-0.029 (0.981)
ln [*KIAA0685*]	-0.319 (0.859)	-0.197 (0.925)
ln [*NRCAM*]	-0.680 (0.223)	-0.588 (0.345)
ln [*SIPA1L2*]	0.623 (0.445)	0.652 (0.490)
ln [*UGCG*]	-0.252 (0.915)	-0.548 (0.842)
ln [*XBP1*]	-0.069 (0.954)	0.195 (0.888)
ε_i	6.005	5.519

[ ], expression level of indicated gene; ( ), p-value. [a]0.000528.

chemotherapy is most commonly used as a post-operative adjuvant therapy for esophageal cancer in Japan, the prediction models for individual clinical response to 5-FU-based chemotherapy, in terms of overall survival (OS) and disease-free survival (DFS), were fixed. The expression levels of the selected marker genes in 14 tumor samples estimated by real-time RT-PCR were used to develop a prediction model and those in subsequently collected 4 tumors were used as test values to confirm the predictive accuracy of the model.

Since expression levels of *DPYD, B4GALT5, UGCG* and *XBP1* correlated with the therapeutic efficacy of 5-FU *in vitro*, we first investigated the correlation of the expression level in tumor samples and clinical response to 5-FU. However, none of the 4 genes alone could accurately predict clinical response to 5-FU therapy, either for OS or DFS. Since CDDP was administered with 5-FU, though at a low dose, we also studied predictive significance of *GSTP1, ARFRP1, IFITM1, KIAA0685* and *SIPA1L2*, which correlated with CDDP sensitivity *in vitro*, and found limited predictive value for each of the 5 genes alone in clinical response to the adjuvant chemotherapy.

In contrast to these findings, application of combined expression data of either of the selected gene sets, 5 genes known as sensitivity determinants or 9 novel highly correlative genes, in 14 tumors in the predictive formulae for OS and DFS yielded the best linear models, and their predictive value was suggested by the consequent utility-confirmation analysis using subsequently analyzed 4 tumor samples (Table III and Fig. 2). We also constructed other potent prediction formulae using different sets of the marker genes, e.g. a set of *GSTP1, ARFRP1, IFITM1* and *KIAA0685*, but their predictive utilities estimated in test samples were not superior to those of the prediction formulae using either a set of the 5 genes or the 9 genes (data not shown).

Discussion

In this study, with a hypothesis that expression analysis of a set of the key drug sensitivity genes could allow us to predict therapeutic response to several active or potent agents in esophageal cancers simultaneously, we attempted to identify potent marker genes for 7 drugs (5-FU, MMC, DOX, CDDP, TXL, TXT, and CPT-11) and an active form of CPT-11, SN-38. We were able to select 5 better marker genes known as drug sensitivity determinants and identify another 9-gene set as novel potent markers for 4 anticancer drugs [5-FU, CDDP, DOX, and CPT-11 (SN-38)] among the target drugs, through 2 different genome-wide microarray analyses and subsequent real-time RT-PCR. Despite the fact that the functional significance of the 9 genes in drug sensitivity is poorly understood, their expression levels were shown to be more highly correlative with cellular sensitivities to the 4 drugs than those of the 5 known drug sensitivity genes. We then determined expression data of the 2 sets of genes quantified by real-time RT-PCR as probable predictors and fixed the best linear model, which embraced the variable expressions of the component genes and arranged them in order to predict the efficacy of the drugs, using multiple regression analysis. These approaches provided 4 and 2 prediction formulae, respectively, for the *in vitro* activity of the 4 drugs and individual clinical responses to 5-FU-based post-operative adjuvant chemotherapy in terms of overall survival and disease free survival in each case, using a set of 5 known or 9 novel genes. All the fixed formulae appeared to be of predictive value, but the models using a set of 9 novel genes are likely to have more advantage in prediction.

We previously showed the first concise prediction models of the *in vitro* activity for 8 drugs (5-FU, CDDP, MMC, DOX, CPT-11, SN-38, TXL, and TXT) using various cancer cell lines, along with individual clinical responses to 5-FU using expression data of 12 genes selected from functionally proven genes alone (11). However, since biological behavior and the molecular basis of cancer differ significantly among cancer origins, it suggests the limited value of the prediction models in esophageal cancer. In fact, the potent marker genes selected in this study largely differed from those shown in our previous study. In the present study, no possible marker genes were suggested for MMC, TXL, or TXT in ESCC. Since they have not yet been approved as therapeutic agents for esophageal cancer, our data may explain the facts that the response of esophageal cancer to anticancer agents is peculiar

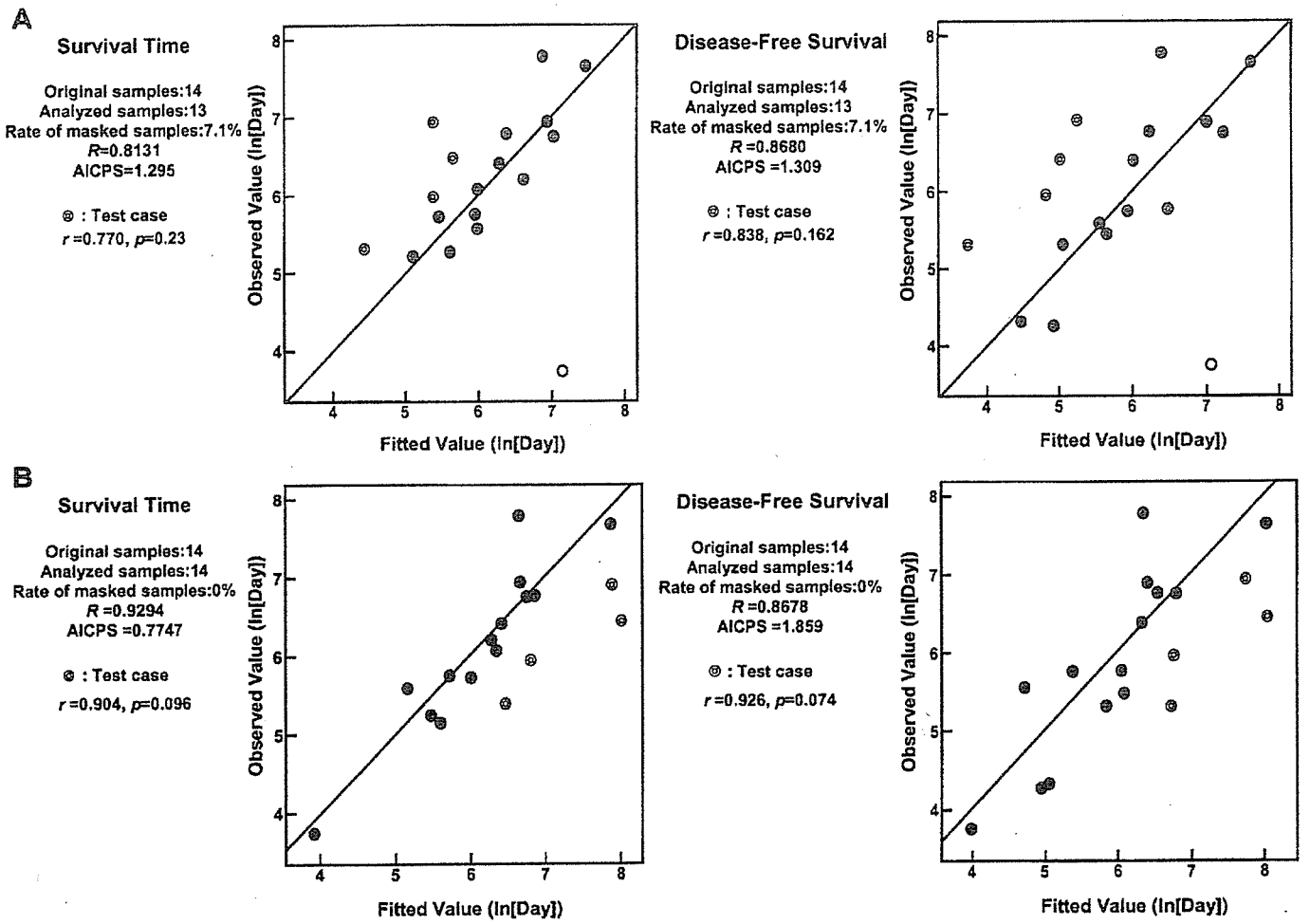

Figure 2. The relationship between observed value and fitted value calculated by fixed formulae for clinical response to 5-FU-based chemotherapy. We also developed formulae to predict the therapeutic efficacy of 5-FU-based chemotherapy, using the variable expression levels of 5 functionally known genes (A) or 9 highly correlative genes with sensitivity to 4 drugs in expression levels (B) which were selected by *in vitro* studies. A total of 14 tumor samples obtained earlier were used as experimental samples to develop a prediction model (a closed circle indicates analyzed sample data, while an open circle indicates a masked outlier), and subsequently obtained 4 samples, as test samples to confirm the predictive accuracy of the development model (double open circle). A vertical axis and a horizontal axis show observed value and fitted value (both are logarithmically transformed), respectively.

among cancers. ESCC probably has prominent prediction markers of its own due to its unique molecular basis.

Very few critical markers, however, have been validated to date for esophageal cancer, although there is clear evidence that a variety of genes are closely associated with cellular sensitivity to anticancer drugs in several cancers (5,38,39). Although comprehensive gene expression analysis using DNA chip is a useful tool for the discovery of prediction markers, there has been no effective way to determine the critical marker genes from a huge number of candidates through expression-sensitivity correlation analysis alone. We can also create a prediction model for sensitivity of esophageal tumors to adjuvant chemotherapy using comprehensive gene expression analysis (40), but the practical value remains unknown. We therefore first determined the selection targets on genes already known as sensitivity determinants. All of the 5 selected genes in this study are considered to be among the most powerful for prediction of responses to the 4 drugs. The correlation of the 5 known genes with drug sensitivity, such as *DPYD* for 5-FU, *BCL2* for DOX, *GSTP1* for CDDP, *XRCC1* for CPT-11, and *MGMT* for SN-38, were confirmed in both comprehensive and quantified gene expression analysis, and numerous model systems and clinical studies have demonstrated their functional significance as indicators of drug sensitivity, even when used alone (18,21,22,27,30-34). Even so, the individual correlation with drug sensitivity was too weak to show potent values as prediction markers.

The biological functions of the 9 newly selected genes (another set of potent prediction markers) remain poorly understood; however, they are more correlative with corresponding drug sensitivity than the 5 known genes in their expression levels. The functions of the 9 genes were little known to date: *ARFRP1* encodes a protein localized in the trans-Golgi network, and may maintain the normal secretory function of the cell; *B4GALT5* is responsible for the synthesis of oligosaccharides in many glycoproteins as well as the carbohydrate moieties of glycolipids; *CALU* encodes a Ca^{2+}-binding protein localized in the endoplasmic reticulum (ER), involved in such ER functions as protein folding and sorting; *IFITM1* has been suggested as playing a role in the anti-proliferative activity of interferons; *NRCAM* encodes a cell adhesion molecule specific to the nervous system and the

molecule modulates neurite outgrowth and guidance via multiple interactions with different proteins; *UGCG* product catalyzes the first glycosylation step in glycosphingolipid biosynthesis; *XBP1* encodes an active transcription factor inducing expression of genes in ER (41-47); the functions of *KIAA0685* and *SIPA1L2* are not known to date. Although the selection approaches differed, these 2 sets of genes (5 known and 9 novel genes) may be better current candidates for prediction markers of drug response in ESCC. We therefore developed prediction models using the expression data of each set of the selected genes.

The fact that drug sensitivity is determined by multiple genes required a better understanding of the intricate network of the selected genes in the expression levels. In the present study, we used multiple regression analysis and reached the prediction formulae of *in vitro* drug activity and clinical response to 5-FU-based chemotherapy, and found that evaluation of the variable expression of the 2 sets of selected genes appeared to work well in the prediction model, even though none of the selected genes alone could accurately predict drug response. It is obvious that practical usefulness needs to be evaluated by a prospective study, but the fixed prediction formulae, especially the formulae using expression data of 9 novel genes, showed high predictive potential. These results suggest that simultaneous performance of two different types of comprehensive gene expression analysis, cDNA and oligonucleotide microarray analyses, may provide a way to identify potent marker genes from the expression-sensitivity correlation analysis alone. We believe our approach is one of the most practical methods available at present to identify more reliable novel prediction markers of drug response. The functional roles of the selected 9 genes in drug sensitivity are the focus of our intensive continuing study.

Nevertheless, in the clinical application models, the key genes in the prediction models somewhat vary from those in an *in vitro* prediction system. We hypothesized that the significance of truly useful genes would not be affected by other unnecessary genes in such a prediction system, which was confirmed in our *in vitro* prediction system but not in the clinical application models. The p-value for each θ_p demonstrated that there was no key gene in the prediction formulae. Although the precise reasons are unclear at present, heterogeneity of the tumor samples and unsettled administered doses of CDDP among patients might have influenced the results. We are now planning a prospective clinical study to clarify the reasons and evaluate the practical value, along with continuing our search for more powerful predictive marker genes for drug sensitivity.

Acknowledgements

We thank Dr Yutaka Shimada (Kyoto University) for his kind supply of 20 KYSE cell lines with helpful advices for the culture. We also thank Chiyo Oda for her technical assistance in MTT assay. Part of this study was supported by Grant from The Science Promotion Fund of the Ministry of Education, Culture, Sports, Science and Technology of Japan, Grant-in-Aid for Scientific Research (B) (2) (no. 14370390, to M.N.) and Grant-in-Aid for University and Industry Collaboration (A) (to M.N.).

References

1. Koshy M, Esiashvilli N, Landry JC, Thomas CR Jr and Matthews RH: Multiple management modalities in esophageal cancer: epidemiology, presentation and progression, work-up, and surgical approaches. Oncologist 9: 137-146, 2004.
2. Ancona E, Ruol A, Santi S, Merigliano S, Sileni VC, Koussis H, Zaninotto G, Bonavina L and Peracchia A: Only pathologic complete response to neoadjuvant chemotherapy improves significantly the long term survival of patients with resectable esophageal squamous cell carcinoma: final report of a randomized, controlled trial of preoperative chemotherapy versus surgery alone. Cancer 91: 2165-2174, 2001.
3. Ando N, Iizuka T, Ide H, Ishida K, Shinoda M, Nishimaki T, Takiyama W, Watanabe H, Isono K, Aoyama N, Makuuchi H, Tanaka O, Yamana H, Ikeuchi S, Kabuto T, Nagai K, Shimada Y, Kinjo Y and Fukuda H: Surgery plus chemotherapy compared with surgery alone for localized squamous cell carcinoma of the thoracic esophagus: a Japan Clinical Oncology Group Study-JCOG9204. J Clin Oncol 21: 4592-4596, 2003.
4. Tak VM and Naunheim KS: Current status of multimodality therapy for esophageal carcinoma. J Surg Res 117: 22-29, 2004.
5. Adlard JW, Richman SD, Seymour MT and Quirke P: Prediction of the response of colorectal cancer to systemic therapy. Lancet Oncol 3: 75-82, 2002.
6. Evans WE and Relling MV: Pharmacogenomics: translating functional genomics into rational therapeutics. Science 286: 487-491, 1999.
7. Iqbal S and Lenz HJ: Targeted therapy and pharmacogenomic programs. Cancer 97: 2076-2082, 2003.
8. Scherf U, Ross DT, Waltham M, Smith LH, Lee JK, Tanabe L, Kohn KW, Reinhold WC, Myers TG, Andrews DT, Scudiero DA, Eisen MB, Sausville EA, Pommier Y, Botstein D, Brown PO and Weinstein JN: A gene expression database for the molecular pharmacology of cancer. Nat Genet 24: 236-244, 2000.
9. McLeod HL and Evans WE: Pharmacogenomics: unlocking the human genome for better drug therapy. Annu Rev Pharmacol Toxicol 41: 101-121, 2001.
10. Staunton JE, Slonim DK, Coller HA, Tamayo P, Angelo MJ, Park J, Scherf U, Lee JK, Reinhold WO, Weinstein JN, Mesirov JP, Lander ES and Golub TR: Chemosensitivity prediction by transcriptional profiling. Proc Natl Acad Sci USA 98: 10787-10792, 2001.
11. Tanaka T, Tanimoto K, Otani K, Satoh K, Ohtaki M, Yoshida K, Toge T, Yahata H, Tanaka S, Chayama K, Okazaki Y, Hayashizaki Y, Hiyama K and Nishiyama M: Concise prediction models of anticancer efficacy of 8 drugs using expression data from 12 selected genes. Int J Cancer 111: 617-626, 2004.
12. Morita T, Togo S, Kubota T, Kamimukai N, Nishizuka I, Kobayashi T, Ichikawa Y, Ishikawa T, Takahashi S, Matsuo K, Tomaru Y, Okazaki Y, Hayashizaki Y and Shimada H: Mechanism of postoperative liver failure after excessive hepatectomy investigated using a cDNA microarray. J Hepatobiliary Pancreat Surg 9: 352-359, 2002.
13. Hiyama K, Otani K, Ohtaki M, Satoh K, Kumazaki T, Takahashi T, Mitsui Y, Okazaki Y, Hayashizaki Y, Omatsu H, Noguchi T, Tanimoto K and Nishiyama M: Differentially expressed genes throughout the cellular immortalization processes are quite different between normal human fibroblasts and endothelial cells. Int J Oncol 27: 87-95, 2005.
14. Ohtaki M, Otani K, Satoh K, Kawamura T, Hiyama K and Nishiyama M: Model-based analysis of microarray data: exploration of differentially expressed genes between two cell types based on a two-dimensional mixed normal model. Jpn J Biometrics 26: 31-48, 2005.
15. Rousseeuw PJ: Least median of squares regression. J Am Statist Assoc 79: 871-880, 1984.
16. Chung YM, Park S, Park JK, Kim Y, Kang Y and Yoo YD: Establishment and characterization of 5-fluorouracil-resistant gastric cancer cells. Cancer Lett 159: 95-101, 2000.
17. Cresteil T, Monsarrat B, Dubois J, Sonnier M, Alvinerie P and Gueritte F: Regioselective metabolism of taxoids by human CYP3A4 and 2C8: structure-activity relationship. Drug Metab Dispos 30: 438-445, 2002.
18. Davis JM, Navolanic PM, Weinstein-Oppenheimer CR, Steelman LS, Hu W, Konopleva M, Blagosklonny MV and McCubrey JA: Raf-1 and Bcl-2 induce distinct and common pathways that contribute to breast cancer drug resistance. Clin Cancer Res 9: 1161-1170, 2003.

19. Diasio RB and Johnson MR: Dihydropyrimidine dehydrogenase: its role in 5-fluorouracil clinical toxicity and tumor resistance. Clin Cancer Res 5: 2672-2673, 1999.
20. Gorrini C, Donzelli M, Torriglia A, Supino R, Brison O, Bernardi R, Negri C, Denegri M, Counis MF, Ranzani GN and Scovassi AI: Effect of apoptogenic stimuli on colon carcinoma cell lines with a different c-myc expression level. Int J Mol Med 11: 737-742, 2003.
21. Goto S, Ihara Y, Urata Y, Izumi S, Abe K, Koji T and Kondo T: Doxorubicin-induced DNA intercalation and scavenging by nuclear glutathione S-transferase π. FASEB J 15: 2702-2714, 2001.
22. Goto S, Kamada K, Soh Y, Ihara Y and Kondo T: Significance of nuclear glutathione S-transferase π in resistance to anticancer drugs. Jpn J Cancer Res 93: 1047-1056, 2002.
23. Grassilli E, Ballabeni A, Maellaro E, Del Bello B and Helin K: Loss of MYC confers resistance to doxorubicin-induced apoptosis by preventing the activation of multiple serine protease- and caspase-mediated pathways. J Biol Chem 279: 21318-21326, 2004.
24. Hayes MC, Birch BR, Cooper AJ and Primrose JN: Cellular resistance to mitomycin C is associated with overexpression of MDR-1 in a urothelial cancer cell line (MGH-U1). BJU Int 87: 245-250, 2001.
25. Hidaka S, Yasutake T, Fukushima M, Yano H, Haseba M, Tsuji T, Sawai T, Yamaguchi H, Nakagoe T, Ayabe H and Tagawa Y: Chromosomal imbalances associated with acquired resistance to fluoropyrimidines in human colorectal cancer cells. Eur J Cancer 39: 975-980, 2003.
26. Iida T, Mori E, Mori K, Goto S, Urata Y, Oka M, Kohno S and Kondo T: Co-expression of gamma-glutamylcysteine synthetase sub-units in response to cisplatin and doxorubicin in human cancer cells. Int J Cancer 82: 405-411, 1999.
27. Knowlton K, Mancini M, Creason S, Morales C, Hockenbery D and Anderson BO: Bcl-2 slows *in vitro* breast cancer growth despite its antiapoptotic effect. J Surg Res 76: 22-26, 1998.
28. Maitra R, Halpin PA, Karlson KH, Page RL, Paik DY, Leavitt MO, Moyer BD, Stanton BA and Hamilton JW: Differential effects of mitomycin C and doxorubicin on P-glycoprotein expression. Biochem J 355: 617-624, 2001.
29. Nishiyama M, Suzuki K, Kumazaki T, Yamamoto W, Toge T, Okamura T and Kurisu K: Molecular targeting of mitomycin C chemotherapy. Int J Cancer 72: 649-656, 1997.
30. Noguchi T, Tanimoto K, Shimokuni T, Ukon K, Tsujimoto H, Fukushima M, Noguchi T, Kawahara K, Hiyama K and Nishiyama M: Aberrant methylation of *DPYD* promoter, *DPYD* expression, and cellular sensitivity to 5-fluorouracil in cancer cells. Clin Cancer Res 10: 7100-7107, 2004.
31. Okamoto R, Takano H, Okamura T, Park JS, Tanimoto K, Sekikawa T, Yamamoto W, Sparreboom A, Verweij J and Nishiyama M: *O(6)*-methylguanine-DNA methyltransferase (MGMT) as a determinant of resistance to camptothecin derivatives. Jpn J Cancer Res 93: 93-102, 2002.
32. Park SY, Lam W and Cheng YC: X-ray repair cross-complementing gene I protein plays an important role in camptothecin resistance. Cancer Res 62: 459-465, 2002.
33. Plo I, Liao ZY, Barcelo JM, Kohlhagen G, Caldecott KW, Weinfeld M and Pommier Y: Association of XRCC1 and tyrosyl DNA phosphodiesterase (Tdp1) for the repair of topoisomerase I-mediated DNA lesions. DNA Repair 2: 1087-1100, 2003.
34. Pourquier P, Waltman JL, Urasaki Y, Loktionova NA, Pegg AE, Nitiss JL and Pommier Y: Topoisomerase I-mediated cytotoxicity of N-methyl-N'-nitro-N-nitrosoguanidine: trapping of topoisomerase I by the O6-methylguanine. Cancer Res 61: 53-58, 2001.
35. Rasheed ZA and Rubin EH: Mechanisms of resistance to topoisomerase I-targeting drugs. Oncogene 22: 7296-7304, 2003.
36. Tani M, Goto S, Kamada K, Mori K, Urata Y, Ihara Y, Kijima H, Ueyama Y, Shibata S and Kondo T: Hammerhead ribozyme against gamma-glutamylcysteine synthetase attenuates resistance to ionizing radiation and cisplatin in human T98G glioblastoma cells. Jpn J Cancer Res 93: 716-722, 2002.
37. Thomas CJ, Rahier NJ and Hecht SM: Camptothecin: current perspectives. Bioorg Med Chem 12: 1585-1604, 2004.
38. Clarke PA, te Poele R, Wooster R and Workman P: Gene expression microarray analysis in cancer biology, pharmacology, and drug development: progress and potential. Biochem Pharmacol 62: 1311-1336, 2001.
39. Watters JW and McLeod HL: Cancer pharmacogenomics: current and future applications. Biochim Biophys Acta 1603: 99-111, 2003.
40. Kihara C, Tsunoda T, Tanaka T, Yamana H, Furukawa Y, Ono K, Kitahara O, Zembutsu H, Yanagawa R, Hirata K, Takagi T and Nakamura Y: Prediction of sensitivity of esophageal tumors to adjuvant chemotherapy by cDNA microarray analysis of gene-expression profiles. Cancer Res 61: 6474-6479, 2001.
41. Akyerli CB, Beksac M, Holko M, Frevel M, Dalva K, Ozbek U, Soydan E, Ozcan M, Ozet G, Ilhan O, Gurman G, Akan H, Williams BR and Ozcelik T: Expression of IFITM1 in chronic myeloid leukemia patients. Leuk Res 29: 283-286, 2005.
42. Burd CG, Strochlic TI and Gangi Setty SR: Arf-like GTPases: not so Arf-like after all. Trends Cell Biol 14: 687-694, 2004.
43. Grumet M: Nr-CAM: a cell adhesion molecule with ligand and receptor functions. Cell Tissue Res 290: 423-428, 1997.
44. Ichikawa S, Sakiyama H, Suzuki G, Hidari KI and Hirabayashi Y: Expression cloning of a cDNA for human ceramide glucosyltransferase that catalyzes the first glycosylation step of glycosphingolipid synthesis. Proc Natl Acad Sci USA 93: 4638-4643, 1996.
45. Paschen W: Endoplasmic reticulum: a primary target in various acute disorders and degenerative diseases of the brain. Cell Calcium 34: 365-383, 2003.
46. Sato T, Furukawa K, Bakker H, van den Eijnden DH and van Die I: Molecular cloning of a human cDNA encoding beta-1,4-galactosyltransferase with 37% identity to mammalian UDP-Gal:GlcNAc beta-1,4-galactosyltransferase. Proc Natl Acad Sci USA 95: 472-477, 1998.
47. Yabe D, Taniwaki M, Nakamura T, Kanazawa N, Tashiro K and Honjo T: Human calumenin gene (CALU): cDNA isolation and chromosomal mapping to 7q32. Genomics 49: 331-333, 1998.

Oncogene (2006) 25, 917–928

www.nature.com/onc

ORIGINAL ARTICLE

Hypoxia selects for high-metastatic Lewis lung carcinoma cells overexpressing Mcl-1 and exhibiting reduced apoptotic potential in solid tumors

N Koshikawa[1,2], C Maejima[1], K Miyazaki[3], A Nakagawara[3] and K Takenaga[1]

[1]Division of Chemotherapy, Chiba Cancer Center Research Institute, Chuoh-ku, Chiba, Japan; [2]Division of Pathology, Chiba Cancer Center Research Institute, Chuoh-ku, Chiba, Japan and [3]Division of Biochemistry, Chiba Cancer Center Research Institute, Chuoh-ku, Chiba, Japan

Low oxygen tension (hypoxia) is a common feature of solid tumors and stimulates the expressions of a variety of genes including those related to angiogenesis, apoptosis and endoplasmic reticulum (ER) stress response. Here we show a close correlation between metastatic potential and the resistance to hypoxia- and ER stress-induced apoptosis among the cell lines with differing metastatic potential derived from Lewis lung carcinoma. An apoptosis-specific expression profiling and immunoblot analyses revealed that the expression of antiapoptotic Mcl-1 increased as the resistance to apoptosis increased. Downregulation of the Mcl-1 expression in the high-metastatic cells by Mcl-1 small interfering RNA increased the sensitivity to hypoxia-induced apoptosis and decreased the metastatic ability. The hypoxia-induced apoptosis was not associated with p53 accumulation, although at present it is not possible to conclude that apoptosis-induced apoptosis is p53-independent. There was no correlation between the expression levels of ER stress-response proteins GADD153, GRP78 and ORP150 and the resistance to hypoxia or ER stresses. *In vitro*, small numbers of the high-metastatic cells overtook the low-metastatic cells after exposure to several rounds of hypoxia and reoxygenation. In solid tumors initially established from equal mixtures, the proportion of the high-metastatic cells to low-metastatic cells was significantly higher in hypoxic areas. Moreover, the high-metastatic cells were overtaking the low-metastatic cells in some of the tumors. Thus, tumor hypoxia and ER stress may provide a physiological selective pressure for the expansion of the high-metastatic cells overexpressing Mcl-1 and exhibiting reduced apoptotic potential in solid tumors.
Oncogene (2006) **25,** 917–928. doi:10.1038/sj.onc.1209128; published online 10 October 2005

Keywords: hypoxia; ER stress; apoptosis; Mcl-1; metastasis

Correspondence: Dr K Takenaga, Division of Chemotherapy, Chiba Cancer Center Research Institute, 666-2 Nitona, Chuoh-ku, Chiba 260-8717, Japan.
E-mail: keizo@chiba-cc.jp
Received 6 January 2005; revised 22 August 2005; accepted 22 August 2005; published online 10 October 2005

Introduction

Response to low oxygen tension (hypoxia) is a fundamental biological phenomenon and therefore hypoxia gives rise to a variety of physiological responses at cellular, local and systemic levels. The cells placed under hypoxic conditions activate many genes including those related to cell survival, glycolysis, angiogenesis, erythrocyte production and iron metabolism to adapt the environment (Semenza, 2000, 2002; Harris, 2002). The oxygen sensing mechanisms have been intensively studied and found to involve hypoxia-inducible factors (HIFs) as key regulatory transcription factors that are composed of HIF-α subunit and HIF-β/aryl hydrocarbon receptor nuclear translocator subunit (Semenza, 2000, 2002; Harris, 2002). HIF binds to the hypoxia-responsive element of hypoxia-responsive genes such as vascular endothelial growth factor (VEGF) and proapoptotic Bnip3, a member of the Bcl-2 family (Semenza, 2000, 2002; Harris, 2002).

Most solid tumors harbor areas of hypoxia, both acute and chronic, due to aberrant vasculature formation and high interstitial pressure (Chaplin and Hill, 1995; Brown and Giaccia, 1998). Although most of the tumor cells die in chronic hypoxia, some of them actually can survive for more than several days in a quiescent or the so-called dormant state (Durand and Sham, 1998) and restart to divide once closed vessels reopen or new vasculatures reach the hypoxic areas. It has been shown that hypoxia induces genetic instability, DNA over-replication and gene amplification in a variety of cultured cells (Rice *et al.*, 1986; Russo *et al.*, 1995; Coquelle *et al.*, 1998). A short-term hypoxia followed by reoxygenation transiently enhances invasive and metastatic potential of some tumor cells (Young and Hill, 1990; Graham *et al.*, 1999; Cairns *et al.*, 2001). Tumor hypoxia selects $p53^{-/-}$ transformed cells and thereby expands cells with diminished apoptotic potential *in vitro* (Graeber *et al.*, 1996). These mechanisms all together are likely to influence the malignant progression of tumor cells (Hill, 1990; Russo *et al.*, 1995; Graeber *et al.*, 1996; Coquelle *et al.*, 1998; Dachs and Chaplin, 1998). Besides, since hypoxic tumor cells cease to divide, they are resistant to conventional radiotherapy and chemotherapy (Rice *et al.*, 1986; Young and Hill, 1990; Teicher, 1994).

Physiological endoplasmic reticulum (ER) stress such as glucose starvation is also present in solid tumors. Hypoxia has been shown to upregulate ER stress-response genes including growth arrest/DNA damage-inducible protein 153 (GADD153/CHOP), which is a proapoptotic transcription factor (Friedman, 1996) and ER chaperones such as glucose-regulated protein (GRP)78/BIP (Munro and Pelham, 1986) and oxygen-regulated protein (ORP)150, which are antiapoptotic proteins (Kuwabara *et al.*, 1996). Upregulation of these ER stress proteins is HIF-independent.

There is accumulating evidence that developing resistance to common apoptotic stimuli is one of the factors that confer high metastatic capability to tumor cells (Glinsky and Glinsky, 1996; McConkey *et al.*, 1996; Bufalo *et al.*, 1997; Glinsky, 1997; Inbal *et al.*, 1997; Shtivelman, 1997; Takaoka *et al.*, 1997; Fernandez *et al.*, 2000; Lowe and Lin, 2000; Wong *et al.*, 2001). The apoptosis-resistant phenotype may be advantageous for tumor cells to survive in the metastatic process. We reported that the high-metastatic clone (A11 cells) established from Lewis lung carcinoma is more resistant to apoptosis induced by serum starvation, hypoxia and glucose deprivation than the low-metastatic clone (P29 cells) (Takasu *et al.*, 1999). However, it remained to be examined whether there is a correlation between metastatic ability and resistance to apoptosis induced by various stresses among various clones with differing metastatic potential. In addition, molecular mechanisms of the apoptosis resistance of the high-metastatic cells remained obscure. We addressed here these points and, furthermore, if hypoxia could act as a physiological selective pressure in solid tumors for the expansion of high-metastatic tumor cells that possess diminished apoptotic potential. The results showed that the high-metastatic Lewis lung carcinoma cell lines are more resistant to hypoxia- and ER stress-induced apoptosis than the low-metastatic cell lines, that the high-metastatic cells overexpress antiapoptotic Mcl-1, and that hypoxia selects for the high-metastatic cells in solid tumors.

Results

Correlation between metastatic potential and resistance to hypoxia- and ER stress-induced apoptosis in the low- and high-metastatic cell lines

To investigate the correlation between susceptibility to hypoxia-induced cell death and metastatic potential, we exposed the five cell lines with differing metastatic potential derived from a mouse Lewis lung carcinoma (metastatic capability; P29 = P34 < C2 < D6 < A11) to hypoxia (~0.1% O_2), corresponding to oxygen concentrations commonly found in solid tumors. Cell death was monitored after culturing the cell lines for 72 h under hypoxia. The results showed that only less than 8% of P29 and P34 cells were viable while about 20% of C2 cells and over 45% of D6 and A11 cells remained viable (Figure 1a). Thus, we observed a tendency where the resistance to hypoxia-induced cell death is correlated with the metastatic ability. The time course showed that hypoxia induced cell death more rapidly in P29 cells than in A11 cells (Figure 1b). Clonogenic assays in which the cells were exposed to hypoxia for 3 or 4 days and then reoxygenated to form colonies also demonstrated that A11 cells survived longer than P29 cells under hypoxic conditions (Figure 1c). The cells positive for annexin V and TUNEL staining increased in hypoxic P29 cells (Figure 1d). An increase in the number of cells exhibiting chromatin condensation and fragmentation as assessed by DAPI staining was also observed in hypoxic P29 cells (0.1 and 26.1% for normoxic and hypoxic P29 cells, respectively) (Figure 1d). In addition, flow cytometric analysis revealed an increase in the percentage of sub-G1 population in these cells (0.7 and 20.6% for normoxic and hypoxic cells, respectively) (Figure 1e). Thus, these data indicate that hypoxic P29 cells were dying through apoptosis. We confirmed that hypoxic A11 cells died of apoptosis based on the same criteria.

To test whether the high-metastatic cell lines are also resistant to ER stresses compared with the low-metastatic cell lines, we treated P29, P34, D6 and A11 cells with chemical ER stress inducers for 2 days and examined their viability. As shown in Figure 2, compared to P29 and P34 cells, D6 and A11 cells were much more resistant to apoptosis induced by tunicamycin (5 μg/ml), brefeldin A (5 μg/ml), thapsigargin (250 nM) and A23187 (1 μM).

Mcl-1 is overexpressed in the high-metastatic cell lines

To find out the genes responsible for the susceptibility to hypoxia-induced apoptosis, we compared the expression profile of apoptosis-related genes among normoxic and hypoxic P29 and A11 cells using a cDNA expression microarray cumulated apoptosis-related genes. The data showed that A11 cells expressed antiapoptotic *Mcl-1* gene at higher levels than P29 cells (not shown). Immunoblot analysis confirmed a higher expression of Mcl-1 in A11 cells than in P29 cells under both normoxic and hypoxic conditions (Figure 3A). We detected two close bands (40 and 37 kDa) on the blots. Since the expressions of the bands were decreased by treatment with Mcl-1 siRNA (see below), the 37 kDa band may be a degradation product of Mcl-1 or, though less likely, a splicing variant of *Mcl-1* gene. It is of note that the cell lines expressed Mcl-1 (40 kDa) at the levels according to the resistance to hypoxia- and other stress-induced apoptosis (Figure 3A and B). Consistent with the recent report that hypoxia enhances Mcl-1 expression in hepatoma HepG2 cells through HIF-1 (Piret *et al.*, 2005), the amount of Mcl-1 was increased by hypoxia in C2, D6 and A11 cells (Figure 3B). Immunohistochemistry for Mcl-1 on the sections prepared from paraffin-embedded P29 and A11 tumors showed a higher expression of Mcl-1 in A11 cells than in P29 cells, indicating that Mcl-1 overexpression is persistent even *in vivo* (Figure 3C).

The expression profiling also showed that hypoxia induced proapoptotic *Bnip3* gene expression in both P29

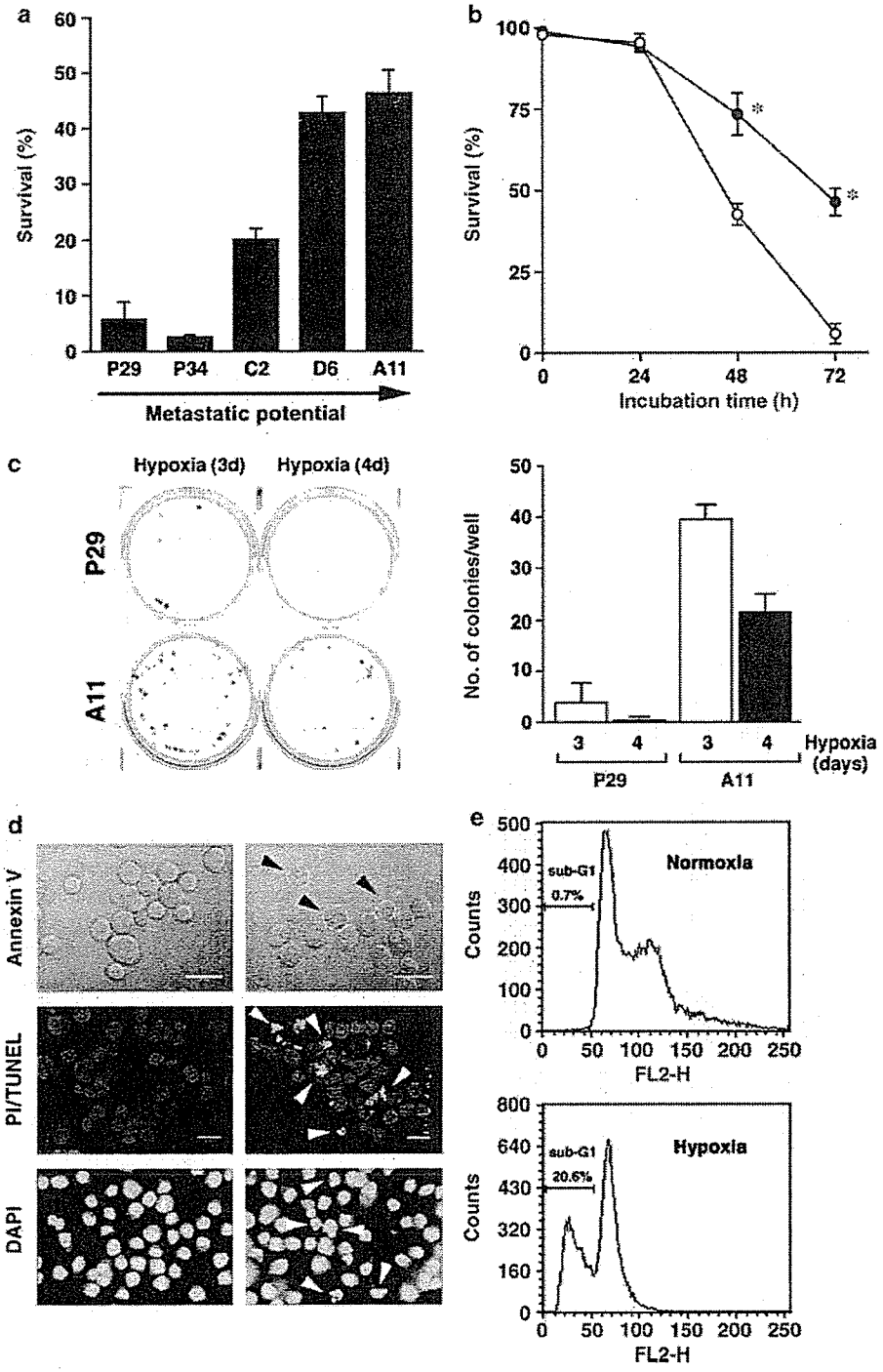

Figure 1 Sensitivity to hypoxia-induced apoptosis of the Lewis lung carcinoma cell lines. (**a**) Hypoxia-induced cell death of the cell lines with differing metastatic potential. The cell lines were exposed to hypoxia for 72 h. Percentage of living cells was determined on the basis of trypan blue exclusion. Bars; s.d. of triplicate determinations. (**b**) Time course of cell death induced by hypoxia. P29 (○) and A11 cells (•) were exposed to hypoxia for the indicated time period. Percentage of living cells was determined on the basis of trypan blue exclusion Bars; s.d. of triplicate determinations. *Significant at $P<0.002$. (**c**) Clonogenic assay of cell survival. P29 and A11 cells (100 cells/well) were cultured under hypoxic conditions for 3 or 4 days followed by culturing under normoxic conditions. Colonies were stained with crystal violet (left panel) and then counted (right panel). Bars; s.d. of triplicate determinations. (**d**) Annexin V, TUNEL and DAPI stainings of normoxic (left panels) and hypoxic P29 cells (right panels). P29 cells were cultured under hypoxic conditions for 18, 27 or 28 h, and then stained for annexin V-EGFP, TUNEL (green) and PI (red), or DAPI, respectively. Arrowheads show apoptotic cells. (**e**) Flow cytometric analysis of DNA fragmentation. P29 cells cultured under hypoxic conditions for 27 h were subjected to FACscan analysis. The percentage of sub-G1 fraction is also shown.

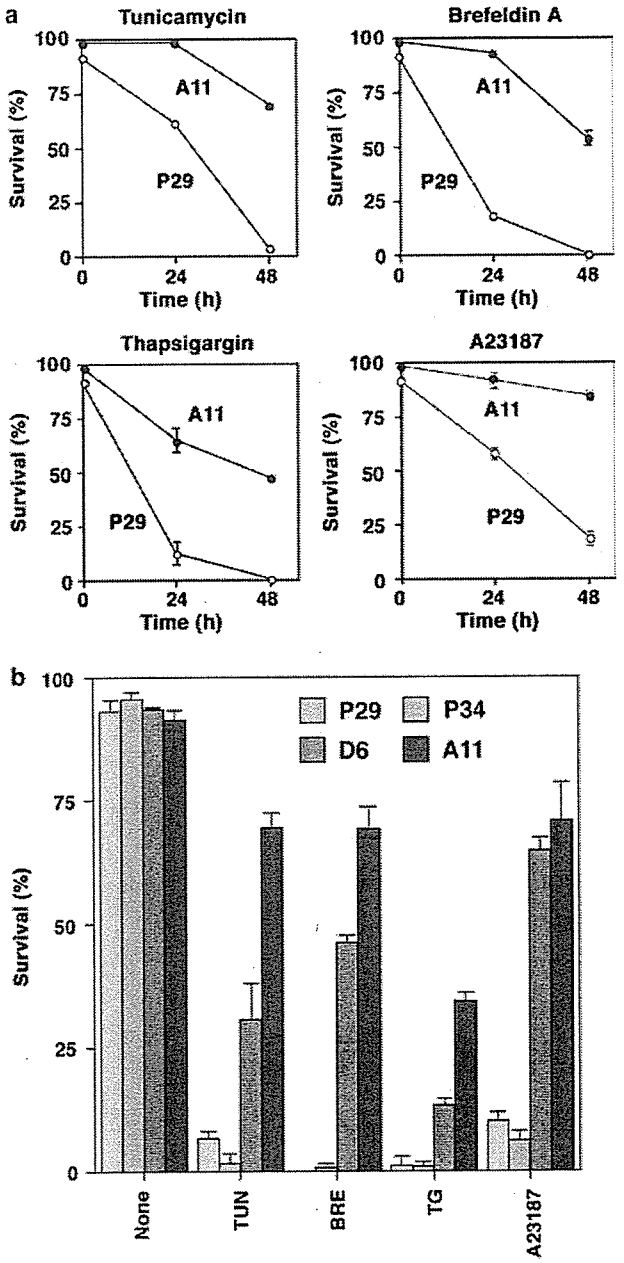

Figure 2 Sensitivity to ER stress-induced apoptosis of the Lewis lung carcinoma cell lines. (**a**) Time course of cell death of P29 (○) and A11 cells (•) exposed to ER stress-inducing agents. The cells were exposed to tunicamycin (5 μg/ml), brefeldin A (5 μg/ml), thaspigargin (250 nM), A23187 (1 μM)). (**b**) Sensitivity of the cell lines with differing metastatic potential to ER stress-inducing agents. P29, P34, D6 and A11 cells were exposed to tunicamycin (5 μg/ml), brefeldin A (5 μg/ml), thaspigargin (250 nM), A23187 (1 μM)) for 2 days. Percentage of living cells was determined on the basis of trypan blue exclusion. Bars; s.d. of triplicate determinations.

and A11 cells (data not shown). Actually, *Bnip3* mRNA expression was induced in all of the cell lines, but the expression level was not correlated with the susceptibility to hypoxia- and other stress-induced apoptosis (Figure 3D).

To investigate whether the hypoxia-induced apoptosis is associated with p53 accumulation, we examined the expression of p53 in hypoxia- and doxorubicin-treated P29, P34, D6 and A11 cells. Immunoblot analysis revealed that hypoxia reduced p53 expression (Figure 3E) and failed to induce endogenous downstream p53 effector proteins, Bax and $p21^{WAF1/CIP1}$, in these cell lines (not shown). By contrast, doxorubicin caused the accumulation of p53 (Figure 3E).

We next compared the expression levels of ER stress-response proteins, GADD153, GRP78 and ORP150, which are known to be induced by hypoxia, between P29 and A11 cells. As shown in Figure 3F and G, the expressions of these proteins were induced by tunicamycin and hypoxia, but there was no difference between 29 and A11 cells.

Effects of Mcl-1 siRNA on hypoxia-induced apoptosis and metastatic potential

To examine if the expression of Mcl-1 is responsible for the resistance to hypoxia-induced apoptosis, we transfected A11 cells with either Mcl-1 siRNA or control siRNA. As shown in Figure 4a and b, the expression of Mcl-1 was suppressed by Mcl-1 siRNA, but not by control siRNA. We then cultured these cells under hypoxic conditions for 60 h and monitored cell death. The results showed that Mcl-1 siRNA-treated A11 cells were more sensitive to hypoxia-induced apoptosis than mock and control siRNA-treated cells in both normal growth medium and serum-starved medium (Figure 4c). Importantly, Mcl-1 siRNA-treated A11 cells were less metastatic than control siRNA-treated cells, as assessed by lung weight and the number of metastatic nodules in the lung (Figure 4d). Thus, it appeared that Mcl-1 is at least in part involved in resistance to hypoxia-induced apoptosis and metastatic potential of A11 cells.

Apoptosis of the low- and high-metastatic cells in hypoxic areas of solid tumors

To examine whether the difference in the susceptibility to hypoxia-induced apoptosis can also be observed *in vivo*, we injected EF5, a nitroimidazole compound, into mice bearing subcutaneous P29 or A11 tumors of nearly equal size for detecting hypoxic areas and stained cryosections of the tumors first with TUNEL assay using fluorescein-labeled nucleotides, and then with Cy3-labeled antibodies against EF5-cellular macromolecule adducts (Figure 5a). EF5 binding occurs under low-oxygen conditions and only in viable cells (Lord *et al*., 1993). The number of TUNEL-positive cells per 100 μm^2 in EF5-positive (hypoxic) and -negative (normoxic) areas was counted (Figure 5b). We omitted necrotic areas from the investigation. The results showed that the number of apoptotic cells in hypoxic areas of P29 tumors was fourfold larger than that in hypoxic areas of A11 tumors. In normoxic areas, the number of apoptotic cells was small but statistically larger in P29 tumors than in A11 tumors.

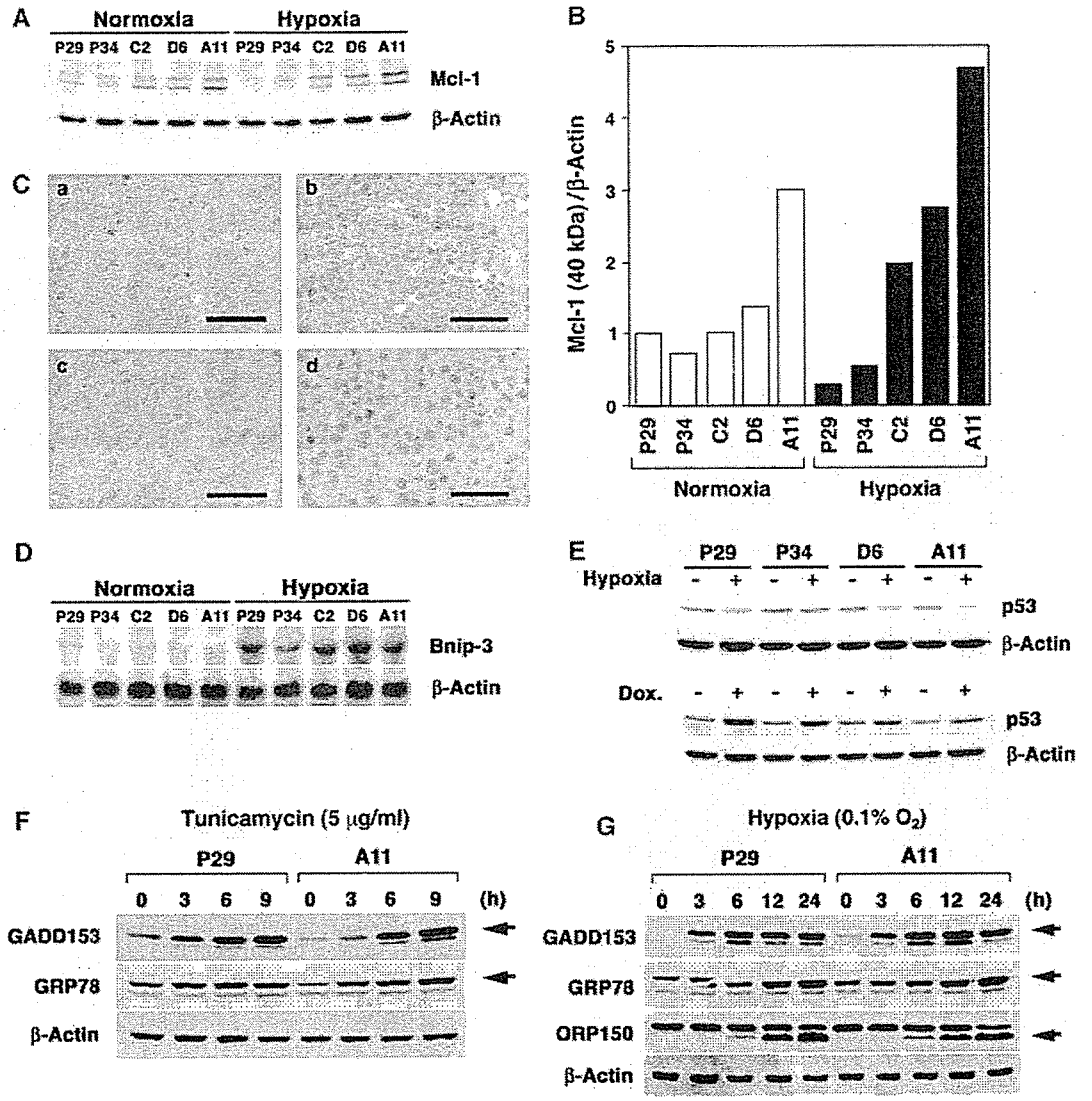

Figure 3 Expressions of apoptosis-related genes in Lewis lung carcinoma cell lines. (**A**) Western blot analysis of the effect of hypoxia on Mcl-1 expression. The cells exposed to hypoxia (~0.1% O_2) for 8 h were subjected to immunoblot analysis for Mcl-1 expression. β-actin served as loading controls. (**B**) Relative values for signal intensity of Mcl-1 (40 kDa) after normalization to the level of β-actin. Scanning densitometry of the gel was performed and the normalized values were represented by the white (under normoxia) and black (under hypoxia) bars. All values are shown as a percentage of the value for normoxic P29 cells. The results are representative of two separate experiments in which similar results were obtained. (**C**) Immunohistochemical analysis of Mcl-1 expression in P29 and A11 tumors. Sections from P29 tumors (a and c) and A11 tumors (b and d) were immunostained with anti-Mcl-1 antibody (a and b) and control IgG (c and d). Bars; 50 μm. (**D**) Effects of hypoxia on *Bnip3* mRNA expression. The cells exposed to hypoxia (0.1% O_2) for 8 h were subjected to Northern analysis for Bnip3 mRNA expression. β-Actin mRNA served as loading controls. (**E**) Western blot analysis of the effects of hypoxia and doxorubicin on the accumulation of p53 protein. The cells exposed to hypoxia (0.1% O_2) for 24 h or 5 μg/ml doxorubicin (Dox) for 20 h were subjected to immunoblot analysis for p53 expression. β-Actin served as loading controls. (**F**) Western blot analysis of the effects of tunicamycin on the expressions of GADD153 and GRP78. P29 and A11 cells were exposed to 5 μg/ml tunicamycin for the indicated periods of time. βActin served as loading controls. (**G**) Western blot analysis of the effects of hypoxia on the expressions of GADD153, GRP78 and ORP150. P29 and A11 cells were exposed to hypoxia (0.1% O_2) for the indicated periods of time. β-actin served as loading controls.

Survival advantage of the high-metastatic cells under hypoxic conditions

The above results prompted us to examine whether A11 cells have a survival advantage over P29 cells under hypoxic conditions. To this end, we established genetically labeled P29 ($P29^{EGFP}$ cells) and A11 cells ($A11^{IRES\text{-}EGFP}$ cells) after selecting P29 and A11 cells stably transfected with pEGFP-N1 and pIRES2-EGFP, respectively (Figure 6a), and characterized their properties. $P29^{EGFP}$ cells grew faster than $A11^{IRES\text{-}EGFP}$ cells *in vivo*, and at 17 days after tumor cell inoculation $P29^{EGFP}$ tumors were twice larger than $A11^{IRES\text{-}EGFP}$ tumors (Figure 6b). $P29^{EGFP}$ tumors contained large necrotic regions. $P29^{EGFP}$ and $A11^{IRES\text{-}EGFP}$ cells were low- and

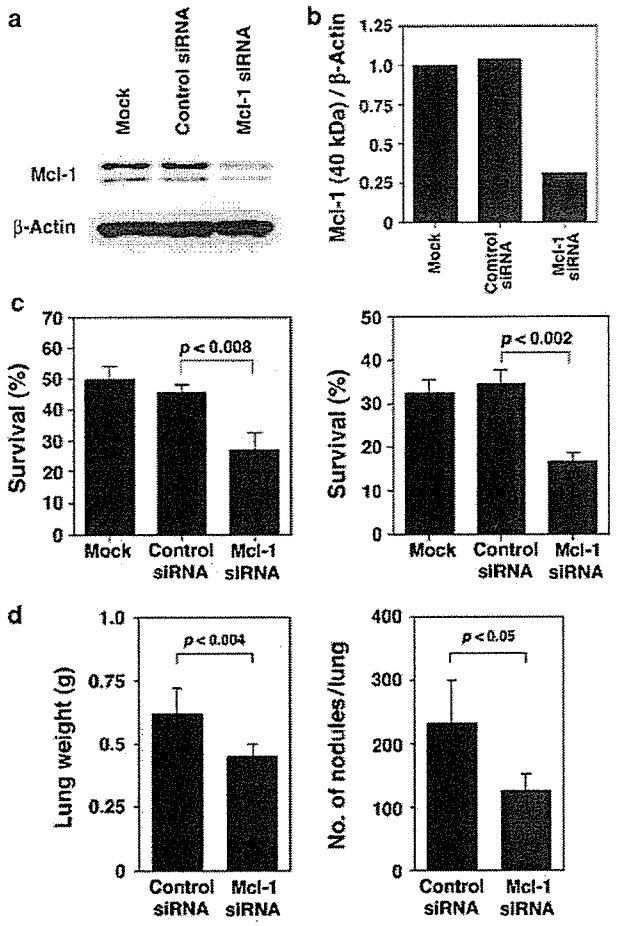

Figure 4 Effects of Mcl-1 siRNA on hypoxia-induced apoptosis and metastatic potential of A11 cells. (**a**) Expression of Mcl-1 in A11 cells treated with Mcl-1 siRNA. A11 cells pretreated with Lipofectamine 2000 alone (mock), 25 nM control siRNA or 25 nM Mcl-1 siRNA for 2 days were subjected to immunoblot analysis for Mcl-1 expression. β-Actin served as loading controls. (**b**) Relative values for signal intensity of Mcl-1 (40 kDa) after normalization to the level of β-actin. Scanning densitometry of the gel was performed and the relative values were represented. All values are shown as a percentage of the value for mock-transfected A11 cells. The results are representative of three separate experiments in which similar results were obtained. (**c**) Sensitivity of Mcl-1 siRNA-treated A11 cells to hypoxia-induced apoptosis. A11 cells pretreated with Lipofectamine 2000 alone (mock), 25 nM control siRNA or 25 nM Mcl-1 siRNA for 2 days were cultured under hypoxic conditions ($\sim$0.1% O_2) for 60 h in normal growth medium (left panel) or serum-starved (1% serum) medium (right panel). Cell death was examined by trypan blue staining. Bars; s.d. of triplicate determinations. (**d**) Metastatic potential of Mcl-1 siRNA-treated A11 cells. A11 cells pretreated with 25 nM control siRNA or 25 nM Mcl-1 siRNA for 2 days were injected intravenously into C57BL/6 mice (6 mice/group). At 17 days after the injection, the weight of the lungs (left panel) and the number of metastatic nodules (right panel) were measured. Bars; s.d.

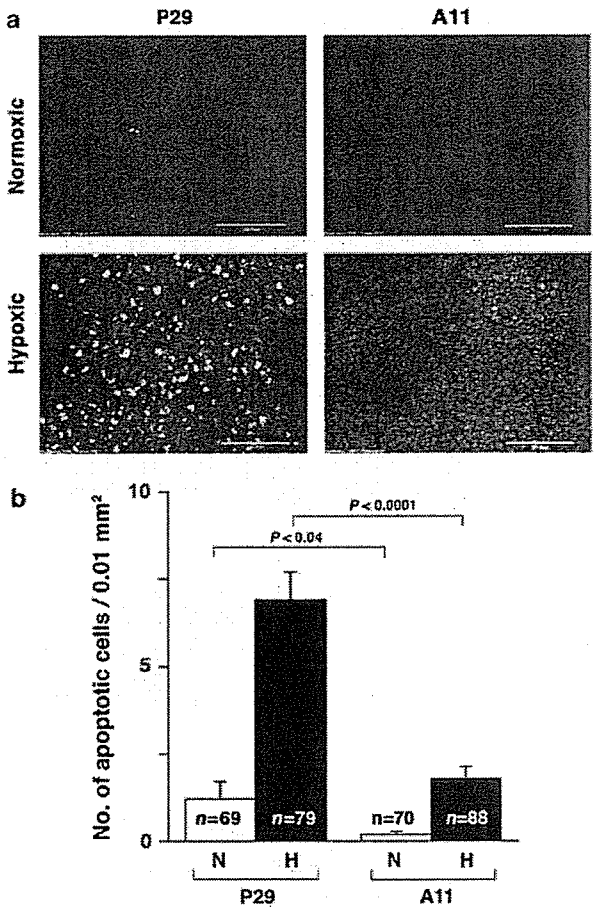

Figure 5 Apoptosis of P29 and A11 cells in tumor hypoxic areas. (**a**) TUNEL staining (green) and EF5 staining (red) of frozen sections of subcutaneous tumors established from P29 and A11 cells. (**b**) Frequency of apoptotic (TUNEL-positive) cells in normoxic (N) and hypoxic (H) areas. Bars; s.e.m.

high-metastatic, respectively, in both experimental and spontaneous metastasis assays (Figure 6c) and showed a similar apoptosis resistance to their parental cells (Figure 6d).

To obtain a standard curve by which the percentage of $A11^{IRES\text{-}EGFP}$ cells in mixtures of unknown proportions of $P29^{EGFP}$ and $A11^{IRES\text{-}EGFP}$ cells could be calculated, we extracted genomic DNA from mixtures of known proportions of the cells and performed PCR followed by Southern blot with an EGFP probe (Figure 6e). By plotting the relative intensities of the bands corresponding to EGFP and IRES-EGFP against the known proportion of $A11^{IRES\text{-}EGFP}$ cells, a standard curve, although slightly sigmoid, was obtained (Figure 6f). The value at each point did not significantly fluctuate even when we carried out PCR under various conditions (1–100 ng DNA, 20–35 PCR cycles) (not shown).

We then mixed $A11^{IRES\text{-}EGFP}$ and $P29^{EGFP}$ cells at a 1:1, 1:10 or 1:100 ratio and treated them with multiple rounds of hypoxia and reoxygenation (recovery in normoxia). The percentage of $A11^{IRES\text{-}EGFP}$ cells at the time of cell harvesting was determined from the standard curve after quantitation of radioactive intensity of the PCR bands. We found that the percentage of $A11^{IRES\text{-}EGFP}$ cells increased dramatically after several rounds of hypoxia-reoxygenation in every case (Figure 7a and b). The intensity of the band corresponding to EGFP and IRES-EGFP in $P29^{EGFP}$ and $A11^{IRES\text{-}EGFP}$

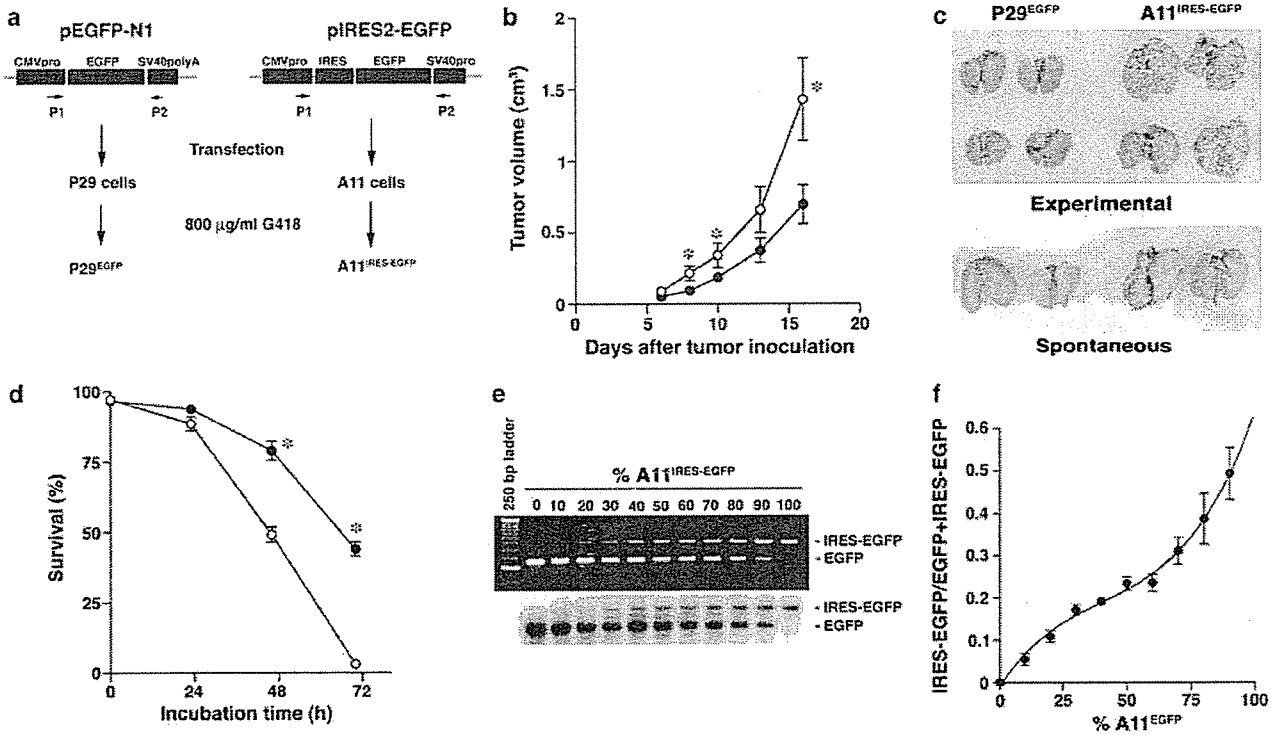

Figure 6 Establishment and properties of $P29^{EGFP}$ and $A11^{IRES\text{-}EGFP}$ cells. (**a**) Schematic drawings of the establishment of $P29^{EGFP}$ and $A11^{IRES\text{-}EGFP}$ cells and the primers, P1 and P2, used for PCR. (**b**) *In vivo* growth of $P29^{EGFP}$ and $A11^{IRES\text{-}EGFP}$ cells. $P29^{EGFP}$ (○) and $A11^{IRES\text{-}EGFP}$ cells (•) (2.5×10^5) were injected subcutaneously into C57BL/6 mice (7 mice/group). Bars; s.e.m. *Significant at $P<0.04$. (**c**) Metastatic potential of $P29^{EGFP}$ and $A11^{IRES\text{-}EGFP}$ cells. For experimental metastasis, the cells (2×10^5 cells/mouse) were injected intravenously, and the lungs were excised 17 days after the injection. For spontaneous metastasis, the cells (2×10^5 cells/mouse) were inoculated subcutaneously, and the lungs were excised 30 days after the inoculation. (**d**) Hypoxia-induced apoptosis of $P29^{EGFP}$ (○) and $A11^{IRES\text{-}EGFP}$ cells (•). Percentage of living cells was determined on the basis of trypan blue exclusion. Bars; s.d. of triplicate determinations. *Significant at $P<0.003$. (**e**) Ethidium bromide staining and Southern blot of PCR fragments amplified using genomic DNA extracted from mixtures of known proportions of $P29^{EGFP}$ and $A11^{IRES\text{-}EGFP}$ cells. (**f**) A standard curve by which the percentage of $A11^{IRES\text{-}EGFP}$ cells in a mixed culture or a tumor could be calculated. The relative intensities of the bands shown in (**e**) were plotted against the known proportion of $A11^{IRES\text{-}EGFP}$ cells. Bars; s.d. of three independent experiments.

cells, respectively, treated with the same protocol was constant (Figure 7c), indicating that the integrated marker genes was stable.

Survival advantage of the high-metastatic cells in solid tumors

We next examined the proportion of $A11^{IRES\text{-}EGFP}$ cells in normoxic and hypoxic areas of solid tumors established from a 1:1 mixture of $P29^{EGFP}$ and $A11^{IRES\text{-}EGFP}$ cells. Since $P29^{EGFP}$ cells grew faster than $A11^{IRES\text{-}EGFP}$ cells *in vivo* (Figure 6b), the percentage of $A11^{IRES\text{-}EGFP}$ cells in both normoxic and hypoxic areas of the heterogeneous tumors should be lower than 50% if no selection of cells occurs in the tumors. We cut out EF5-negative and -positive areas (approximately total 1 mm^2) from cryosections of the tumors excised at 17 days after tumor inoculation by using laser-assisted microdissection, extracted genomic DNA, and then examined the percentage of $A11^{IRES\text{-}EGFP}$ cells in these areas as described above (Figure 8a and b). The data showed that the proportion of $A11^{IRES\text{-}EGFP}$ cells in normoxic areas decreased from the initial 50% in five out of the seven mixed tumors. However, the proportion was over 70% in #2 and #5 tumors (Figure 8b). Intriguingly, the percentage of $A11^{IRES\text{-}EGFP}$ cells in hypoxic areas was quite high in five out of the seven tumors. Overall, the proportion of $A11^{IRES\text{-}EGFP}$ cells in normoxic and hypoxic areas was 36.4 ± 26.0 and $69.0 \pm 21.0\%$, respectively ($P<0.011$). The intensity of bands corresponding to EGFP and IRES-EGFP of the cells collected from normoxic and hypoxic areas of $P29^{EGFP}$ and $A11^{IRES\text{-}EGFP}$ tumors was constant (Figure 8c), indicating that the integrated marker genes was also stable *in vivo*. Thus, $A11^{IRES\text{-}EGFP}$ cells showed a clear survival advantage over $P29^{EGFP}$ cells in hypoxic areas.

The loss of $P29^{EGFP}$ cells in normoxic areas of some heterogeneous tumors (#2 and #5 tumors) suggests a possibility that a greater portion of $P29^{EGFP}$ cells was lost in the tumors. To test this possibility, we extracted genomic DNA from the whole tumors and examined the proportion of $A11^{IRES\text{-}EGFP}$ cells. The results showed that the proportion was over 90% in #2 tumor, indicating that $A11^{IRES\text{-}EGFP}$ cells nearly overtook $P29^{EGFP}$ cells in this tumor (Figure 8d and e). In #5 tumor, it was below 50%. This and the above results suggest that $A11^{IRES\text{-}EGFP}$

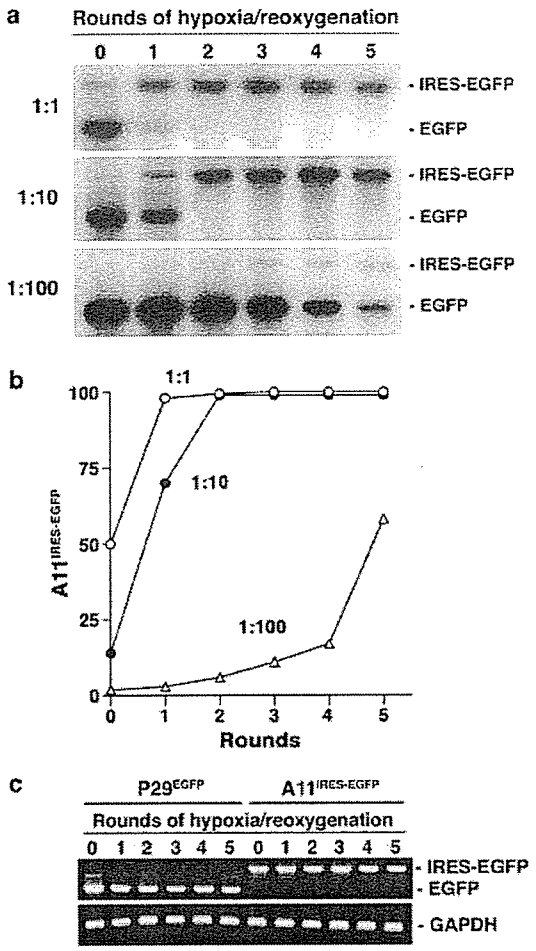

Figure 7 Hypoxia-reoxygenation selects $A11^{IRES\text{-}EGFP}$ cells in a mixed culture. (**a**) Southern blot of PCR fragments amplified using genomic DNA extracted from mixtures of $P29^{EGFP}$ and $A11^{IRES\text{-}EGFP}$ cells. $A11^{IRES\text{-}EGFP}$ were mixed with $P29^{EGFP}$ cells at a 1:1, 1:10 or 1:100 ratio and treated with multiple rounds of hypoxia-reoxygenation. (**b**) Selection of $A11^{IRES\text{-}EGFP}$ cells following hypoxia-reoxygenation treatment. The percentage of $A11^{IRES\text{-}EGFP}$ cells was calculated by the standard curve shown in Figure 6f after measuring the relative intensities of the PCR bands shown in (**a**). The data are representative of two separate experiments in which similar results were obtained. (**c**) Stability of the integrated marker genes in $P29^{EGFP}$ and $A11^{IRES\text{-}EGFP}$ cells. Ethidium bromide staining of the PCR bands is shown.

cells nearly overtook $P29^{EGFP}$ cells only in the local normoxic areas that were dissected by microdissection. The percentage of $A1^{IRES\text{-}EGFP}$ cells was over 50% in #1 and #6 tumors, suggesting that the cells were overtaking $P29^{EGFP}$ cells in these tumors. In other 3 tumors, the percentage was below 50%, indicating that selection of $A11^{IRES\text{-}EGFP}$ cells was occurring in local hypoxic areas of these tumors but was not apparent in whole tumor mass.

Discussion

The data presented here showed a close correlation between metastatic potential and the resistance to hypoxia-induced apoptosis among the cell lines with differing metastatic potential. They also showed that the high-metastatic cells are more resistant to ER stress-induced apoptosis. The hypoxia-induced apoptosis may be p53-independent, because hypoxia neither caused p53 accumulation nor induced the expressions of endogenous downstream p53 effector proteins. An apoptosis-specific expression profiling and immunoblot analyses demonstrated a correlation between the resistance to hypoxia-induced apoptosis and the expression level of Mcl-1. Downregulation of the Mcl-1 expression in A11 cells by Mcl-1 siRNA increased the sensitivity to hypoxia-induced cell death and, importantly, decreased the metastatic ability. Although there are so far few reports directly indicating the involvement of Mcl-1 in metastatic potential of tumor cells, a clinicopathological study suggested Mcl-1 as an indicator of tumor progression and prognosis in patients with gastric carcinoma (Maeta *et al*., 2004). Therefore, Mcl-1 may be one of the factors that confer metastatic potential on at least some tumor cells.

In agreement with the previous reports (Bruick, 2000; Guo *et al*, 2001), hypoxia induced the expression of Bnip3 in all of the cell lines used in this study. Bnip3 is a mitochondrial protein and induces apoptosis independently of Apaf-1, cytochrome *c* release and caspase activation (Vande Velde *et al*., 2000). Bcl-2 and Bcl-X_L bind to Bnip3 and inhibit apoptosis caused by the overexpression of Bnip3 (Ray *et al*., 2000). Therefore, it is possible that Mcl-1 binds to Bnip3 and inhibits Bnip3-induced apoptosis. We preliminarily examined this possibility, and the data showed that Mcl-1 physically interacts with Bnip3 (data not shown).

There was no difference in the inducibility of ER stress- and hypoxia-inducible genes such as GADD153, GRP78 and ORP150 genes between the low- and the high-metastatic cell lines, eliminating the involvement of these genes in the difference of the sensitivity to hypoxia- and ER-stress-induced apoptosis.

The present results clearly demonstrated the survival advantage of A11 cells over P29 cells. In the mixed culture, A11 cells overtook P29 cells during several rounds of hypoxia-reoxygenation. It would be of interest to note that as the rounds of selection proceeded A11 cells progressively became more resistant to apoptosis induced by not only hypoxia but also serum starvation, glucose deprivation and anticancer drugs such as cisplatin and etoposide (not shown). Therefore, it is likely that repeated exposure to hypoxia-reoxygenation results in the selection of not merely A11 cells with original phenotype but of A11 cells with more malignant phenotype, consistent with previous reports (Kim *et al*., 1997; Kinoshita *et al*., 2001).

Coinciding with the *in vitro* experiments, the frequency of apoptosis was greater in the hypoxic areas of A11 tumors than in those of P29 tumors. Intriguingly, it appeared that A11 cells became a majority in the hypoxic areas of many tumor masses established from equal mixtures of P29 and A11 cells. It is of note that although we randomly excised the hypoxic areas the proportion of A11 cells in these areas was over 90% in

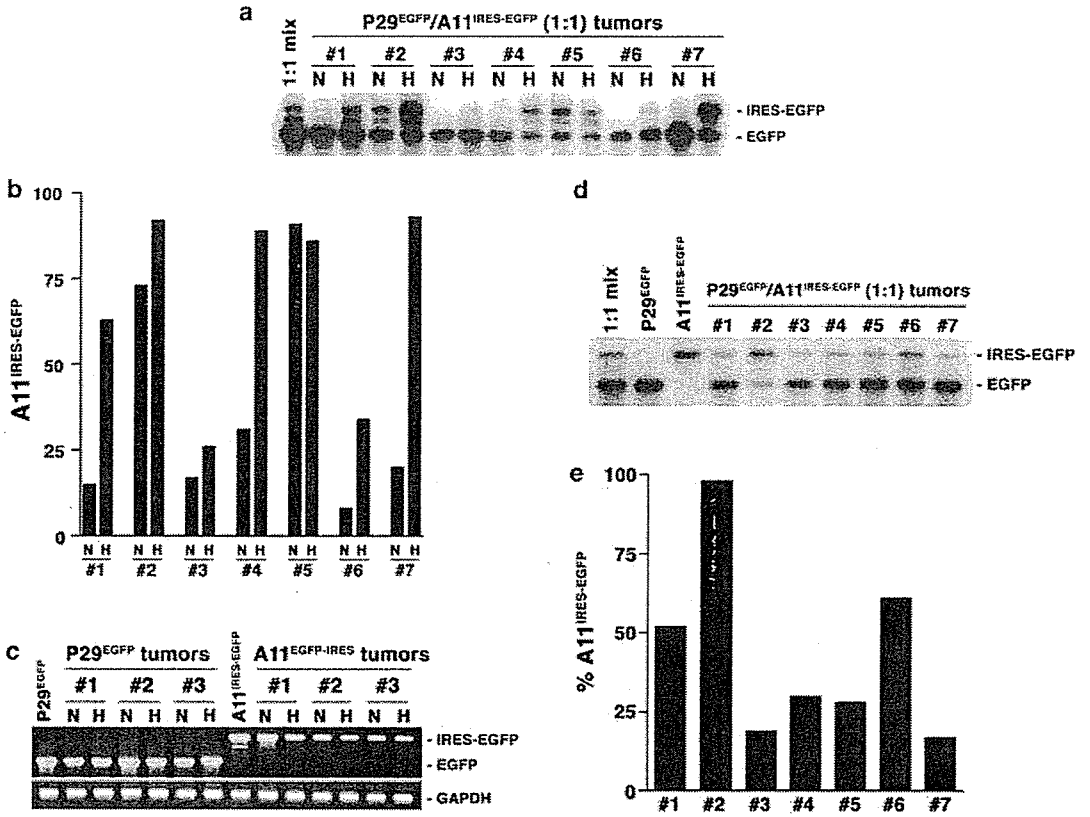

Figure 8 Proportion of A11$^{IRES\text{-}EGFP}$ cells in tumors. (**a**) Southern blot of PCR fragments amplified using genomic DNA extracted from normoxic (N) and hypoxic (H) areas in subcutaneous tumors established from equal mixtures of P29^{EGFP} and A11$^{IRES\text{-}EGFP}$ cells. (**b**) The percentage of A11$^{IRES\text{-}EGFP}$ cells in normoxic (N) and hypoxic (H) areas in subcutaneous tumors. The percentage of A11$^{IRES\text{-}EGFP}$ cells was calculated by the standard curve shown in Figure 5f after measuring the relative intensities of the PCR bands shown in (**a**). (**c**) Stability of the integrated marker genes in normoxic (N) and hypoxic (H) areas of P29^{EGFP} and A11$^{IRES\text{-}EGFP}$ tumors. Ethidium bromide staining of the PCR bands is shown. (**d**) Southern blot of PCR fragments amplified using genomic DNA extracted from subcutaneous tumors established from equal mixtures of P29^{EGFP} and A11$^{IRES\text{-}EGFP}$ cells. (**e**) The percentage of A11$^{IRES\text{-}EGFP}$ cells in subcutaneous tumors. The percentage of A11$^{IRES\text{-}EGFP}$ cells was calculated by the standard curve shown in Figure 6f after measuring the relative intensities of the PCR bands shown in (**d**). Tumor numbers (#) correspond to those in (**a**).

several samples. This was somewhat surprising. We had expected that the proportion would vary widely from one sample to another, because the time of hypoxia influences the degree of apoptosis and EF5-binding does not tell us how long hypoxia had lasted in EF5-positive areas before excision. Nevertheless, a majority of P29 cells was commonly lost in the randomly selected hypoxic areas. One possible explanation for this is that P29 cells die more rapidly in *in vivo* hypoxic areas in which starvation of growth factors and nutrients that could act synergistically with hypoxia to induce apoptosis also occurs. We then exposed P29 and A11 cells to serum starvation (0.5% FBS) and hypoxia (0.1% O_2) simultaneously. The data showed that more than 75% of P29 cells died within 24 h while more than 70% of A11 cells survived. Thus, P29 cells are less tolerant towards severer conditions in *in vivo* hypoxic areas than A11 cells, and this might explain the rapid loss of P29 cells in hypoxic areas. Interestingly, we observed two cases out of the seven tumors in which A11 cells dominated in not only hypoxic areas but also normoxic areas. It is possible that the normoxic areas represent the ones that are reoxygenated after hypoxia. Intriguingly, in one case (#2 tumor), the proportion of A11 cells in the tumor mass was over 90%. This suggests that a majority of P29 cells died of apoptosis induced by severe hypoxia and other microenvironmental factors in the early phase of growth of this tumor, resulting in the selection of A11 cells. The degree of tumor vascularization and angiogenesis may vary from one tumor to another even if they are established from the same tumor cells, and accordingly the extent of hypoxia may differ in individual tumor. This may explain the difference in the proportion of A11 cells in each tumor.

It has been reported that hypoxia induces p53-dependent apoptosis and thus selects $p53^{-/-}$ cells (Graeber *et al.*, 1996). Our study showed that hypoxia selects for cells with reduced apoptotic potential and high-metastatic ability. This phenomenon could occur in human tumors such as cervical cancer, head and neck cancer and soft tissue sarcoma in which a correlation between hypoxia and aggressiveness or poor prognosis has been reported (Brizel *et al.*, 1996, 1997; Höckel

et al., 1996, 1999). Therefore, the data presented here may have important implications for malignant progression of tumors.

Materials and methods

Cell culture
The cell lines, P29, P34, C2, D6 and A11, established from Lewis lung carcinoma, have been characterized elsewhere (Takasu *et al.*, 1999; Koshikawa *et al.*, 2003). They were grown in Dulbecco's modified Eagle's medium (DMEM) containing 10% fetal bovine serum supplemented with 100 units/ml penicillin and 100 μg/ml streptomycin. Cells were cultured at 37°C in a humidified atmosphere with 5% CO_2 or under hypoxic conditions (ca. 0.1% O_2) generated in BBL GasPak Pouch (Becton Dickinson Microbiology Systems, Cockeysville, MA, USA). In some experiments, they were treated with tunicamycin (Sigma-Aldrich, St Louis, MO, USA), brefeldin A (WAKO Pure Chemical Industries, Ltd., Osaka, Japan), thapsigargin (Sigma-Aldrich), A23187 (Sigma-Aldrich) or vehicle alone.

Assessment of cell viability and apoptosis
Cells were seeded at a concentration of 3×10^5 cells/dish (Falcon 3002), and cell death was induced by culturing them under hypoxic conditions or in the presence of various drugs. For aerobic recovery, the cells were cultured in normoxia until they become subconfluent, thus the recovery time was different for each cell line. Cell viability was assessed by trypan blue dye exclusion. Flow cytometric analysis was performed as described previously (Takasu *et al.*, 1999) to detect cellular DNA fragmentation with a FACScan flow cytometer (Becton Dickinson, Mountain View, CA, USA). Chromatin condensation and fragmentation were visualized by staining the cells with DAPI (10 μg/ml). Annexin V and terminal deoxynucleotidyl transferase-mediated deoxyuridine triphosphate nick-end labeling (TUNEL) stainings were carried out using Annexin V-EGFP Apoptosis Detection Kit (MBL, Nagoya, Japan) and ApopTag Fluorescein *In situ* Apoptosis Detection Kit (Serologicals Corp., Norcross, GA, USA), respectively, according to the manufacturer's instructions. The fluorescence was observed under a Fluoview confocal laser microscope (Olympus, Tokyo, Japan). For clonogenic assay, cells were seeded at a concentration of 100 cells/well of six-well plates (Falcon 3046), incubated for 3 or 4 days under hypoxic (~0.1% O_2) conditions, and then allowed to grow under normoxic conditions for 8–10 days. Colonies were fixed with methanol and stained with 0.05% crystal violet.

Expression profiling of apoptosis-related genes
Expressions of apoptosis-related genes in normoxic and hypoxic P29 and A11 cells were carried out using Mouse Apoptosis GEArray Q™ series containing a panel of 96 key genes involved in apoptosis (SuperArray, Inc., Bethesda, MD, USA). Hybridization of the microarray with a biotin-16-dUTP-labeled cDNA probe and chemiluminescent detection were performed according to the manufacturer's instructions.

Northern blot analysis
Total RNA was electrophoresed on 1% agarose gel containing formaldehyde and transferred to nylon filters. Blots were hybridized with a ^{32}P-labeled mouse *Bnip3* cDNA probe that was prepared by RT–PCR.

Small interfering RNA (siRNA) transfection
Mcl-1 siRNA (Santa Cruz Biotechnologies, Inc., Santa Cruz, CA, USA) or Silencer Negative Control #1 siRNA (Ambion, Inc., Austin, TX, USA) was transfected into A11 cells with Lipofectamine 2000 (Invitrogen, Carlsbad, CA, USA) according to the manufacturer's protocol. At 3 days after transfection, the cells were subjected to immunoblot analysis for Mcl-1 expression, apoptosis assay and metastasis assay.

Immunoblot analysis
Cells were lysed in 1% Triton X-100, 1% sodium deoxycholate, 0.1% SDS, 50 mM Tris-HCl, pH 7.5, 150 mM NaCl, 1 mM PMSF and protease inhibitor cocktail (Sigma-Aldrich) or directly dissolved in SDS sample buffer. After centrifugation at 10 000 *g* for 10 min at 4°C, the supernatant was used for immunoblot analysis. Proteins were separated by SDS–PAGE under reducing conditions and transferred to a nitrocellulose membrane. The membrane was incubated with first antibodies, washed extensively with TBS-T, and then with species-appropriate HRP-conjugated secondary antibodies. The first antibodies used were anti-p53 antibody (Ab-3, Calbiochem-Novabiochem, Germany), anti-Mcl-1 antibody (Santa Cruz Biotechnology, Inc.), anti-GADD153 antibody (Santa Cruz Biotechnology, Inc.), anti-GRP78 antibody (Santa Cruz Biotechnology, Inc.), anti-ORP180 antibody (IBL, Fujioka, Japan) and anti-β-actin antibody (Sigma-Aldrich). Immunodetection was performed using the enhanced chemiluminescence system (ECL; Amersham Biosciences Corp., Piscataway, NJ, USA). The image of the bands was acquired with an imaging densitometer, and the signal intensities were analyzed with an NIH Image 1.63 software on a Machintosh computer. All signals were normalized to β-actin.

Tumor growth and metastasis assays
Cells (2×10^5 cells/mouse) were inoculated into the abdominal flank of age-matched female C57BL/6 mice (Nippon SLC, Hamamatsu, Japan). Subcutaneous tumor growth was monitored by caliper measurement of two diameters at right angles, and the tumor mass was estimated from the equation volume $= 0.5 \times a \times b^2$, where a and b are the larger and smaller diameters, respectively. For spontaneous metastasis assay, the mice were killed 30 days after tumor cell inoculation, and their lungs were removed. For experimental metastasis assay, tumor cells (2×10^5 cells/mouse) were injected intravenously, and the lungs were removed 17 days later. The lungs were fixed in Bouin's solution and the parietal metastatic nodules were counted. All animal experiments were performed in compliance with the institutional guidelines for the care and use of laboratory animals.

Immunohistochemistry
Subcutaneous tumors were excised, fixed in 10% buffered formalin and embedded in paraffin wax. Paraffin sections were cut at 6 μm thickness and mounted on the silane-coated glass slides. After routine dewaxing and rehydrating, the sections were incubated in 1 × ChemMate®Target Retrieval Solution (DakoCytomation, Glostrup, Denmark) at 121°C for 15 min and rinsed with Dulbecco's phosphate-buffered saline (DPBS). For quenching endogenous peroxidase activity, the sections were incubated in 0.3% H_2O_2 in methanol for 30 min. Thereafter, they were incubated with diluted normal goat serum for 20 min at room temperature and then incubated with anti-Mcl-1 antibody or normal rabbit IgG (4 μg/ml) diluted in ChemMate® Antibody Diluent (DaKoCytomation) containing 2% dry milk at 4°C for 16 h. Immunostaining was carried out by using VECTASTAIN® ABC Kit according to the

manufacturer's instructions. The sections were washed with DPBS and finally counterstained with hematoxylin.

Detection and microdissection of hypoxic areas in tumors
In all, 300 μl of EF5 solution (3 mg/ml) was injected intraperitoneally into mice bearing subcutaneous tumors (Inbal *et al.*, 1997). After 1 h, tumors were surgically removed and frozen in OCT compound. Cryostat sections cut at 10 μm were fixed with 4% paraformaldehyde and washed with DPBS. The sections were treated with 5% mouse serum, 20% dry milk and 0.3% Tween 20 in DPBS overnight at 4°C to block nonspecific binding sites. They were rinsed with 0.3% Tween 20 in DPBS and then incubated with Cy3-labeled monoclonal anti-EF5 antibody (ELK3-51) for 4 h at 4°C. After extensive washing with DPBS, tissue samples were observed under a confocal laser microscope or a fluorescence microscope. For detection of apoptotic cells *in vivo*, TUNEL staining was performed followed by EF5 staining. In some experiments, EF5 binding-positive (hypoxic) and adjacent EF5 binding-negative (normoxic) areas in tumor tissues were dissected using a laser-assisted microdissection system (Leica Microsystems, Tokyo, Japan).

Establishment of cells transfected with pEGFP-N1 or pIRES2-EGFP plasmid
P29 and A11 cells were transfected with pEGFP-N1 and pIRES2-EGFP (BD Biosciences Clontech, Tokyo, Japan), respectively, using Lipofectin reagent (Invitrogen, Tokyo, Japan). After selecting the transfected P29 or A11 cells in the presence of 800 μg/ml G418, a clone designated $P29^{EGFP}$ or $A11^{IRES\text{-}EGFP}$, respectively, was established. They were routinely cultured in the presence of 400 μg/ml G418.

DNA isolation, PCR and Southern blotting
Genomic DNA was extracted from $P29^{EGFP}$, $A11^{IRES\text{-}EGFP}$, mixed cells, solid tumors or microdissected sections by conventional method, treated with RNase A (10 μg/ml) and phenol extracted again. PCR was performed using 1–100 ng genomic DNA and *r*Taq DNA polymerase (TOYOBO Biochemicals, Osaka, Japan) on a Perkin Elmer GeneAmp PCR System 9700. The sense primer (P1) was 5′-AAC TCCGCCCCATTGACGC-3′ corresponding to the sequence within the CMV promoter, and the antisense primer (P2) was 5′-ACAAACCACAACTAGAATGCAG-3′ corresponding to the sequence in the SV40polyA signal. These primers were designed to amplify the EGFP sequence in pEGFP-N1 plasmid and the IRES-EGFP sequence in pIRES2-EGFP plasmid, thus yielding 1118 and 1693 bp PCR products, respectively. The PCR conditions were 94°C for 3 min, followed by 20–30 cycles of 94°C for 30 s, 55°C for 30 s and 72°C for 1 min. The resulting PCR products were electrophoresed on 1.2% agarose gels, transferred to nylon membranes and hybridized with a ^{32}P-labeled *EGFP* cDNA. The membranes were washed and radioactive intensity corresponding to the EGFP and IRES-EGFP bands was quantitated using a Fluoro Image Analyzer FLA-5000 (FUJIFILM, Tokyo, Japan). The measured percentage of $A11^{IRES\text{-}EGFP}$ cells was determined by dividing the intensity of the IRES-EGFP band by the total intensity of the EGFP plus IRES-EGFP bands. The actual percentage of $A11^{IRES\text{-}EGFP}$ cells in a mixed culture and in a tumor was determined from a standard curve established from Figure 6f.

Acknowledgements
We thank the National Cancer Institute (CTEP) for providing EF5. This work was supported in part by Grant-in-Aid from the Ministry of Health, Labour, and Welfare for Third Term Comprehensive Control Research for Cancer and from the Ministry of Education, Culture, Sports, Science and Technology.

References

Brizel DM, Scully SP, Harrelson JM, Layfield LJ, Bean JM, Prosnitz LR *et al.* (1996). *Cancer Res* **56**: 941–943.
Brizel DM, Sibley GS, Prosnitz LR, Scher RL, Dewhirst MW. (1997). *Int J Radiat Oncol Biol Phys* **38**: 285–289.
Brown JM, Giaccia AJ. (1998). *Cancer Res* **58**: 1408–1416.
Bruick RK. (2000). *Proc Natl Acad Sci USA* **97**: 9082–9087.
Bufalo DD, Biroccio A, Leonetti C, Zupi G. (1997). *FASEB J* **11**: 947–953.
Cairns RA, Kalliomaki T, Hill RP. (2001). *Cancer Res* **61**: 8903–8908.
Chaplin DJ, Hill SA. (1995). *Br J Cancer* **71**: 1210–1213.
Coquelle A, Toledo F, Stern S, Bieth A, Debatisse M. (1998). *Mol Cell* **2**: 259–265.
Dachs GU, Chaplin DJ. (1998). *Semin Radiat Oncol* **8**: 208–216.
Durand RE, Sham E. (1998). *Int J Radiat Oncol Biol Phys* **42**: 711–715.
Fernandez Y, Espana L, Manas S, Fabra A, Sierra A. (2000). *Cell Death Differ* **7**: 350–359.
Friedman AD. (1996). *Cancer Res* **56**: 3250–3256.
Glinsky GV. (1997). *Crit Rev Oncol Hematol* **25**: 175–186.
Glinsky GV, Glinsky VV. (1996). *Cancer Lett* **101**: 43–51.
Graeber TG, Osmanian C, Jacks T, Housman DE, Koch CJ, Lowe SW *et al.* (1996). *Nature* **379**: 88–91.
Graham CH, Forsdike J, Fitzgerald CJ, Macdonald-Goodfellow S. (1999). *Int J Cancer* **80**: 617–623.
Guo K, Searfoss G, Krolikowski D, Pagnoni M, Franks C, Clark K *et al.* (2001). *Cell Death Differ* **8**: 367–376.
Harris AL. (2002). *Nat Rev* **2**: 38–47.
Hill RP. (1990). *Cancer Metastasis Rev* **9**: 137–147.
Höckel M, Schlenger K, Aral B, Mitze M, Schaffer U, Vaupel P. (1996). *Cancer Res* **56**: 4509–4515.
Höckel M, Schlenger K, Höckel S, Vaupel P. (1999). *Cancer Res* **59**: 4525–4528.
Inbal B, Cohen O, Polak-Charcon S, Kopolovic J, Vadai E, Eisenbach L *et al.* (1997). *Nature* **390**: 180–184.
Kim CY, Tsai MH, Osmanian C, Graeber TG, Lee JE, Giffard RG *et al.* (1997). *Cancer Res* **57**: 4200–4204.
Kinoshita M, Johnson DL, Shatney CH, Lee YL, Mochizuki H. (2001). *Int J Cancer* **91**: 322–326.
Koshikawa N, Iyozumi A, Gassmann M, Takenaga K. (2003). *Oncogene* **22**: 6717–6724.
Kuwabara K, Matsumoto M, Ikeda J, Hori O, Ogawa S, Maeda Y *et al.* (1996). *J Biol Chem* **271**: 5025–5032.
Lord EM, Harwell L, Koch CJ. (1993). *Cancer Res* **53**: 5721–5726.
Lowe SW, Lin AW. (2000). *Carcinogenesis* **21**: 485–495.
Maeta Y, Tsujitani S, Matsumoto S, Yamaguchi K, Tatebe S, Kondo A *et al.* (2004). *Gastric Cancer* **7**: 78–84.
McConkey DJ, Greene G, Pettaway CA. (1996). *Cancer Res* **56**: 5594–5599.
Munro S, Pelham HR. (1986). *Cell* **46**: 291–300.

Piret JP, Minet E, Cosse JP, Ninane N, Debacq C, Raes M *et al.* (2005). *J Biol Chem* **280**: 9336–9344.
Ray R, Chen G, Vande Velde C, Cizeau J, Park JH, Reed JC *et al.* (2000). *J Biol Chem* **275**: 1439–1448.
Rice GC, Hoy C, Schimke RT. (1986). *Proc Natl Acad Sci USA* **83**: 5978–5982.
Russo CA, Weber TK, Volpe CM, Stoler DL, Petrelli NJ, Rodriguez-Bigas M *et al.* (1995). *Cancer Res* **55**: 1122–1128.
Semenza GL. (2000). *Crit Rev Biochem Mol Biol* **35**: 71–103.
Semenza GL. (2002). *Trends Mol Med* **8**: S62–S67.
Shtivelman E. (1997). *Oncogene* **14**: 2167–2173.
Takaoka A, Adachi M, Okuda H, Sato S, Yawata A, Hinoda Y *et al.* (1997). *Oncogene* **14**: 2871–2977.
Takasu M, Tada Y, Wang JO, Tagawa M, Takenaga K. (1999). *Clin Exp Metastasis* **17**: 409–416.
Teicher BA. (1994). *Cancer Metastasis Rev* **13**: 139–168.
Vande Velde C, Cizeau J, Dubik D, Alimonti J, Brown T, Israels S *et al.* (2000). *Mol Cell Biol* **20**: 5454–5468.
Wong CW, Lee A, Shientag L, Yu J, Dong Y, Kao G *et al.* (2001). *Cancer Res* **61**: 333–338.
Young SD, Hill RP. (1990). *J Natl Cancer Inst* **82**: 371–380.

Zeitschrift EJ ej814
DOI 10.1055/s-2006-924640
Satzbetrieb Ziegler + Müller
Verlag Thieme/Mündel
Datum 18.09.2006

S. Suita
T. Tajiri
M. Higashi
S. Tanaka
Y. Kinoshita
Y. Takahashi
K. Tatsuta

Insights into Infant Neuroblastomas Based on an Analysis of Neuroblastomas Detected by Mass Screening at 6 Months of Age in Japan

Abstract

Background/Purpose: Mass screening (MS) for neuroblastoma (NB) at 6 months of age in Japan was discontinued in 2004. We have previously reported that the majority of NB detected by MS showed a good prognosis, with only a few cases demonstrating an unfavorable outcome (■J Pediatr Surg 2002; Cancer 2001). This study aims to provide insights into infant NB by assessing the details of the clinical courses in patients treated with a standard regimen and the biological features of such cases using highly sensitive methods at one institution in Japan. **Methods:** In 76 NB detected through MS treated at Kyushu University Hospital, the clinical features and *MYCN* amplification, 1p deletion, 17q gain, the expression level of *TrkA* using FISH and the quantitative PCR were analyzed. **Results:** Of these 76 persons with NB treated at one institution, 97% are still alive, while 2 cases died from other diseases. Three patients experienced a recurrence after complete remission (CR), and 2 patients demonstrated refractory disease since the initial diagnosis. Two of the 3 NB patients with recurrence have demonstrated a 2nd CR, while one case still has multiple active diseases. Regarding the findings of highly sensitive biological analyses, 5/74 (7%) showed *MYCN* amplification, 2/24 (8%) cases had a 1p deletion, 3/33 (9%) cases had a 17q gain, 5/50 (10%) cases had diploidy, 1/25 (4%) cases had a low expression of *TrkA*, and 2/76 (3%) cases had an unfavorable histology. Of the 76 NB, 13 tumors (17%) had one or more UF. Of the 5 refractory NB, 1 case had 3 UF, 1 case had 2 UF, 1 case had 1 UF, and 2 cases had no UF. As a result, 60% of the refractory NB had one or more UF. **Conclusions:** Of the NB detected by MS at one institution in Japan, 17% had one or more ■UF and might have a higher risk of recurrence than the patients with no UF, although the unfavorable biology of several refractory cases is still unclear even after highly sensitive analyses. At least one-fifth of the NB cases detected by MS are anticipated cases. In infantile neuroblastomas, it may therefore be most important to analyze biologically prognostic factors using highly sensitive methods followed by immediate surgical intervention. Since the MS program has been discontinued in Japan, it will be necessary in future to assess the mortality and characteristics of NB detected clinically.

Key words
Infantile neuroblastoma · mass screening · biology

Résumé

■ *we complete*

Affiliation
Department of Pediatric Surgery, Graduate School of Medical Sciences, Kyushu University, Fukuoka, Japan

Correspondence
Sachiyo Suita, M.D., Ph.D., FACS (Hon) · Director of Kyushu University Hospital · 3-1-1 Maidashi · Higashi-ku · Fukuoka 812-8582 · Japan · E-mail: suita@pedsurg.med.kyushu-u.ac.jp

Received: August 12, 2005 · **Accepted after Revision:** September 12, 2005

Bibliography
Eur J Pediatr Surg 2006; 16: 1–6 © Georg Thieme Verlag KG Stuttgart · New York · DOI 10.1055/s-2006-924640 · ISSN 0939-7248